

# Malware Epidemic Effects in a Kinetic Conflict Model

Joachim Draeger, Stephanie Öttl

*IABG mbH, Ottobrunn, Germany*

## Abstract

We propose a framework for examining the effects of infections with self-replicating malware on military forces engaged in kinetic combat. The framework uses models, in which kinetic attrition is represented by a Lanchester model coupled with an SIR-like model describing the malware propagation across the forces. Basic knowledge about the expected circumstances restricts the set of scenarios to be analyzed using the model. Remaining uncertainties are taken into account as random variations given by information-theoretic principles. The situation assessment is realized by Monte-Carlo simulations with the risk as a possible assessment measure.

An application of the proposed framework to a simple exemplary situation demonstrates its usage in practice. The assumed uncertainties about the considered situation lead to an outcome statistics, which changes corresponding to the improving knowledge about the situation. Large uncertainties may lead to results profoundly different from point estimates. For assuring practicability, the paper provides options to determine the values of important model parameters by measurement. It also discusses how to utilize the assessment results calculated with help of the framework.

## 1 Introduction

Among all threats related to cyber security, self-replicating malware, like viruses and worms, are some of the most important ones. Due to the capability of self-reproduction, the initial infection of a single, unimportant system component may cause catastrophic damage to the overall system at the end. The disproportionality between the low effort and the potentially significant damage qualifies the usage of malware for large scale attacks and cyber warfare [23, 41]. Indeed, the Cyber Conflict Studies Association CCSA<sup>1</sup> lists numerous incidents at national level. We mention some examples: In 1998, the NATO attacked infrastructure and command & control structures in Serbia during the Kosovo war with self-replicating malware [21], enabling an especially successful air campaign. In April 2007, Estonia was attacked at cyber level, presumably by Russia [8]. The attack has targeted ministries, banks, and media and caused injuries due to riots resulting from the effectiveness of the attack. Trojans have enforced a temporary shutdown of the computer network of the German Bundestag in 2015 [37, 49]. Other examples of attacks with self-replicating malware can be found in [9, 19, 33, 42].

An adequate analysis of malware infection effects must take the (non-)availability of functionalities into account. The degradation of the availability caused by the malware infection leads to a natural loss function and allows an objective and quantitative assessment of the malware effects. This paper considers a conventional battle (i.e. kinetic combat) between two opposing military forces as an exemplary system that has been affected by malware. A Lanchester model is used to describe the two forces and the kinetic combat between them. The propagation of malware across the forces is represented by a SIR-like epidemic model. The analysis of the malware effects on system availability is executed in a framework allowing the portrayal of specific situations by individual models. This contributes to the flexibility of the proposed approach, which paves the way towards a more faithful representation of real world situations. The framework also takes into account that the common idealistic anticipation of perfect knowledge is not always met in practice. Instead, it expresses missing knowledge as epistemic uncertainties. Simulation runs can

<sup>1</sup><http://www.cyberconflict.org>

be used for analyzing the model behavior. When organized in a Monte Carlo method, the sampling of simulation runs can also take uncertainties into account. The approach can especially be used for risk assessments.

Several papers are considering co-occurring kinetic combat and cyber warfare with malware. Mishra and Prajapati [40] discuss cyber warfare based on a differential equation system, but they do not take availability aspects into account; instead, they focus on a stability analysis. McMorrow [38] aims at developing a deeper understanding of large scale cyber attacks based on a comparison of biological and malware epidemics. Schramm [47] has developed a corresponding model combining a kinetic battle situation with a one-sided malware attack based on the SIR model [30]. Its symmetrization by Yildiz [60] assures that both forces have the same capabilities and vulnerabilities. Both [61] and [60] examine and expand the models of Schramm.

The paper is structured as follows. The class of models used in our framework for the investigation of malware effects is presented in section 2. A simple homogeneous model belonging to this class is discussed as an example in section 3. Section 4 develops our concept of a simulation-based computational analysis. The method for including uncertainties is elaborated in this section as well. Section 5 analyzes an exemplary situation with help of the framework, whereby the model of section 3 is reused. These considerations are supplemented by section 6, which discusses the application of the framework from the practice point of view. The paper closes with an outlook in section 7.

## 2 An Integrated Kinetic-Cyber Model

### 2.1 Modeling Strategy

Due to specific circumstances like individual force structures and malware attack vectors, the usage of an 'universal' representation will be doomed to failure. Individual models are required for adapting the model to the situational characteristics. Thus, a *framework* is proposed, in which the underlying model  $M \in \mathcal{M}$  can be chosen from a model class  $\mathcal{M}$ . The restriction to models belonging to  $\mathcal{M}$  assures essential model properties like the fading dynamics for  $t \rightarrow \infty$  in proposition 3 (see section 2.7 below).

The framework is built on the work of Schramm [47] and Yildiz [60]. Accordingly,  $\mathcal{M}$  consists of (generalized) system dynamics models composed of two main components: First, a submodel  $M_K$  representing kinetic combat — or, at least, the corresponding attrition — by a Lanchester-like model [10], and, second, a submodel  $M_C$  representing cyber combat by a SIR-like model [12] of malware epidemics. The experience gained so far confirms that the system dynamics paradigm allows a discussion of basic mechanisms and foundational aspects. Concerning Lanchester, one may take a look at e.g. [10] and references therein. An application to a more recent conflict is given in [29]. Concerning malware epidemics, the realism of compartmental models is discussed in [12]. The system dynamics approach may be overstrained, though, when aiming at precise quantitative predictions. Both kinetic combat and cyber warfare are essentially ill-defined [11, 12, 31, 56]. The ill-definedness is caused by the unpredictability of individual human decisions and by the potential occurrence of unexpected events. Therefore, just relying on more advanced models will not bring about a higher predictive quality compared to simpler models. Additionally, simple models have some principal advantages. Their small computational complexity, for example, enables the sampling of large numbers of simulation runs — we will make use of this option in section 4.3.

### 2.2 The Kinetic Component of the Model

Kinetic combat is modeled using Lanchester equations [32,36], which consider two opposing forces Blue and Red. Since the technical systems used in military forces have usually quite different capabilities and vulnerabilities, heterogeneous Lanchester models [10] are permitted. Although the correspondence between Lanchester model and real system may only be approximate, the basic idea of Lanchester models to reduce the dynamics of combat to attrition rates is notwithstanding considered as a useful concept [1]. Accordingly, Lanchester attrition models are used as components of more encompassing models of kinetic combat [2, 45].

In the kinetic component, all model parameters can be chosen individually for Blue and Red. This is indicated by an index  $b$  resp.  $r$ . Since the effectiveness  $\delta_{ij}$  of an attacking force element is not only determined by its own capabilities, but also by the capabilities of the defender, the model parameters depend on the weapon system types  $i, j$  of both attacker and defender. Accordingly, a general form of the heterogeneous Lanchester model is

$$\begin{aligned}\frac{db_j}{dt} &= \sum_{i=1}^n -\delta_{r,ij} r_i^{p_{r,ij}}(t) b_j^{q_{r,ij}}(t) \\ \frac{dr_j}{dt} &= \sum_{i=1}^n -\delta_{b,ij} b_i^{p_{b,ij}}(t) r_j^{q_{b,ij}}(t)\end{aligned}\tag{1}$$

with  $j = 1, \dots, n$  and initial conditions  $b_j(0), r_j(0) \geq 0$ . In these equations,  $b_j(t)$  resp.  $r_j(t)$  represents the number of the blue resp. red force elements of type  $j$  at time  $t$ . The parameters  $p_{b/r,ij}$  determine the capabilities of the forces as an attacker, whereas  $q_{b/r,ij}$  do so for the defender. Equation system (1) is well-defined unless one of  $r_j$  or  $b_j$  becomes zero during the evolution. This problem is discussed in more detail in section 2.6.

Following the idea of Lanchester's model, each set of force elements represented by an  $r_j$  or  $b_j$  should behave homogeneously concerning attrition. The heterogeneity of the model will thus typically respect the organizational structure of the involved forces. We may also take their spatial arrangement into account in order to distinguish between the parts of the forces that are engaged and those, which are not [16]. Range-dependent attrition rates due to restrictions of the firing range of weapons can be encoded as well [27].

### 2.3 The Cyber Component of the Model

The cyber component  $M_C$  describes the malware propagation across a force by an SIR-like model. Kermack & McKendrick [30] developed the SIR model originally for the description of biological epidemics, but later it was successfully applied to the propagation of malware (e.g. [39, 51, 53]) as well. The notation reflects the three different infection states  $S, I, R$  of the model representing Susceptible (here called vulnerable), Infected, and Recovered (here called patched) force elements. The model assumes that a vulnerable element in contact with an infected individual may become infected itself with a rate  $\beta$ . Infected elements may be patched with a rate  $\bar{\gamma}$ , being immune against the used malware afterwards. This leads to the following equations system of the basic SIR-model:

$$\begin{aligned}\frac{dS}{dt} &= -\beta S(t)I(t) \\ \frac{dI}{dt} &= \beta S(t)I(t) - \bar{\gamma}I(t) \\ \frac{dR}{dt} &= \bar{\gamma}I(t)\end{aligned}\tag{2}$$

Concerning initial conditions, it holds  $S(0), I(0), R(0) \geq 0$ . In the proposed framework, refinements [12, 44, 51] of the SIR model such as the SEIR model [57] may be used. The large potential variety of cyber components corresponds to the large spectrum of possible infection and propagation mechanisms [47]. If required, the cyber model component may be provided for each weapon system type individually; this option will not be elaborated further, though.

The general form of the cyber component is described as a compartmental system. Each compartment  $C_g$ ,  $g = 1, \dots, m$  represents a specific malware infection state of a weapon system. We identify  $C_g$  with the number of force elements being in the state represented by  $C_g$ . These numbers are changing due to flows  $\phi_{gl}(C)$  from  $C_g$  to  $C_l$  dependent on  $C := (C_1, \dots, C_m)$ . The flows portray malware propagation as well as malware removal and other countermeasures for fighting the malware epidemics. The dynamics is thus given by a system

$$\frac{dC_l}{dt} = \sum_{g=1}^m \phi_{gl}(C)\tag{3}$$

of differential equations with  $C_g(t) \geq 0$  for all times  $t \geq 0$  and the values of  $C_g(0)$  [46] as initial conditions. For being well-defined, we assume that all flows  $\phi_{gl}$  are bounded. Of course,

not every term that meets the given technical constraints will describe a malware propagation process in a realistic way. The constraints are necessary, however, to ensure the proper function of the framework. Antisymmetry  $\phi_{gl} = -\phi_{lg}$  assures that the outflow of the stock of force elements in infection state  $g$  given by  $\phi_{gl}$  equals the inflow of the stock of elements in state  $l$ . This means that the compartmental system (3) is closed, i.e. that the population  $\sum_g C_g(t)$  summed up over all states  $g$  is constant over time  $t$ . For preserving this property after integrating kinetic and cyber submodels, i.e. in presence of an annihilation of force elements due to kinetic combat, we assume normalized compartment levels  $C_g(t) = \tilde{C}_g(t)/(\sum_g C_g(t))$ . This assures  $\sum_g C_g(t) = 1$ . Correspondingly, flow terms describing malware propagation processes have to preserve normalization, whereas for flows related to other processes the absolute numbers of force elements are of interest. Accordingly, a normalization has to be omitted for the latter. The example of a kinetic-cyber model presented in section 3 demonstrates an application of the normalization rule.

## 2.4 The Coupling of the Model Components

In the overall model, kinetic and cyber component are coupled with each other for taking the degradation of kinetic capabilities by the propagating malware into account. A malware infection may lead both to a reduced effectiveness of attacking force elements [47, 60] and to a higher loss rate of defending force elements. For representing these effects, additional indices  $k, l$  are introduced as malware infection states of attacker and defender. The kinetic effectivenesses  $\delta_{ikjl}$  have to be chosen correspondingly. This leads to a Lanchester equation system with extended parameterization. Concerning the levels  $b_{jl}$  and  $r_{jl}$  of the force elements of weapon system type  $j$ , the infection state  $l$  is indicated as well. Accordingly, the kinetic interaction term for Blue has the form

$$\mathcal{K}_{b,jl} := - \sum_{i=1}^n \sum_{k=1}^m \delta_{r,ikjl} \cdot r_{ik}^{p_{r,ikjl}}(t) \cdot b_{jl}^{q_{r,ikjl}}(t). \quad (4)$$

The corresponding term for Red is designated as  $\mathcal{K}_{r,jl}$ . We define the numbers of existing force elements according to

$$N_{b,j}(t) := \sum_{l=1}^m b_{jl}(t) \quad \text{and} \quad N_{r,j}(t) := \sum_{l=1}^m r_{jl}(t) \quad (5)$$

We also define an overall force size  $N_{b/r}(t) := \sum_{j=1}^n \zeta_j N_{b/r,j}(t)$  with  $\zeta_j > 0$  as positive summation weights. Using the weights, different levels of importance can be distinguished; an aircraft carrier, for example, contributes more to the overall force than a small patrol boat.

For including the evolving malware propagation (and the fight against it) in the equation system (1), flow terms  $\phi_{b/r,glj}$  are added representing the transitions between the malware infection states  $g$  and  $l$  for the specific weapon system type  $j$ . As for equation (3), we assume that all flow terms  $\phi_{b/r,glj}$  are bounded for reasons of well-definedness. The malware propagation terms are, thus,

$$\mathcal{P}_{b,jl} := \sum_{g=1}^m \phi_{b,glj}(b_{j1}, \dots, b_{jm}) \quad (6)$$

for Blue and  $\mathcal{P}_{r,jl}$  for Red, respectively.

The initial malware infection starting the malware epidemic is caused by a malware attack of the adversarial force. The effect of a malware attack triggered by red force elements of type  $i$  in malware infection state  $k$  on blue force elements of type  $j$  in state  $g$  is represented by a flow

$$\mathcal{A}_{b,jl} := \sum_{i=1}^n \sum_{k=1}^m \sum_{g=1}^m \alpha_{r,ikjgl}(r_{ik}, b_{j1}, \dots, b_{jm}) \quad (7)$$

for Blue and, analogously, by  $\mathcal{A}_{r,jl}$  for Red. The blue force elements being attacked are subject to a state transition  $g \rightarrow l$ . Correspondingly, an antisymmetry condition  $\alpha_{b/r,ikjgl} = -\alpha_{b/r,ikjlg}$  holds in analogy to  $\phi$ . Again, we assume that all flow terms  $\alpha_{b/r,ikjgl}(r_{ik}, b_{j1}, \dots, b_{jm})$  are

bounded for reasons of well-definedness. The precise shape of  $\alpha$  depends on the infection mechanism used by the malware. Examples are given in [47]. The attack rate  $\alpha_{b/r,ikjgl}$  is equal to zero, if the malware infection state  $k$  prohibits a malware attack on enemy force elements or if the weapon system type  $i$  has no malware attack capability. Taken together, this gives the following equation system.

$$\begin{aligned}\frac{db_{jl}}{dt} &= \mathcal{K}_{b,jl} + \mathcal{P}_{b,jl} + \mathcal{A}_{b,jl} \\ \frac{dr_{jl}}{dt} &= \mathcal{K}_{r,jl} + \mathcal{P}_{r,jl} + \mathcal{A}_{r,jl}\end{aligned}\quad (8)$$

We assume non-negativity  $b_{jl}(0), r_{jl}(0) \geq 0$  of all compartments as initial condition. The equation system can be extended by the annihilation losses  $D'_j(t) = -\sum_l \mathcal{K}_{jl}(t)$  for bookkeeping purposes with  $D_j(0) \geq 0$  as initial condition. Additionally, we define  $D(t) := \sum_j \zeta_j D_j(t)$ .

## 2.5 Adding an Event Mechanism

We permit a finite number of timed events modifying parameter values of equation system (8). This extension completes the construction of the underlying model class  $\mathcal{M}$ . In general, the event mechanism can be used for representing various kinds of singular events and for a temporal structuring of the course of action [5, 20, 52, 58]. An exemplary temporal structuring may consist, say, of a preparation, an assault, and an exploitation phase. In these phases, different force elements will have prominent roles. Accordingly, the values of the attrition coefficients will usually differ in the individual phases [24, 27]. We will make use of events in section 3.3 for choosing individual start times of the kinetic combat, of the malware attacks, and of the patching actions.

A typical example of a singular event is a change of the force elements opposing each other due to troop movements [1]. Such re-assignments can be represented by events activating and deactivating attrition between units. Indeed, the Lanchester model is only a model of attrition, but not a full model of combat [50]. It is the event mechanism, which extends the component  $M_K$  from a model of attrition to a general model of kinetic combat. Though several important aspects of conflict have to be taken into account outside of (13), their effects can usually be incorporated in our model by events as additional input. These aspects include not only rather elementary activities like troop movements, but the decisions of the involved military leaders in general. We let the user of the framework experiment with them based on corresponding what-if assumptions.

## 2.6 Model Consistency

The kinetic interaction terms  $\delta_{r,ikjl} \cdot r_{ik}^{p_r,ikjl}(t) \cdot b_{jl}^{q_r,ikjl}(t)$  and  $\delta_{b,ikjl} \cdot b_{ik}^{p_b,ikjl}(t) \cdot r_{jl}^{q_b,ikjl}(t)$  in (8) require further discussion. In order to improve readability, the indices  $i, j, k, l$  are omitted in this section in the following. For  $q_r \rightarrow 0$ , one gets  $b^{q_r}(t) \rightarrow 1$  independently of the value of  $b$ . This means, the losses inflicted on  $b(t)$  by Red become independent of the current size of  $b(t)$ . For  $b$  close to 0, the level of  $b$  thus becomes negative. Similarly, for  $p_r \rightarrow 0$  the term  $r^{p_r}$  becomes approximately equal to 1 independently of the value of  $r$ . Thus, a red force already annihilated can inflict arbitrarily large losses on Blue. For  $p_r = 1, q_r = 1$ , which is the special case usually discussed in literature, such irregularities do not occur.

For avoiding unphysical behavior, a barrier function  $f(x) = (\exp(-1/x))^{0.0001}$  is introduced with  $f(x) \rightarrow 0$  for  $x \rightarrow 0$  and  $f(x) \approx 1$  otherwise. Replacing the original term

$$\delta_r \cdot r^{p_r}(t) \cdot b^{q_r}(t) \quad (9)$$

by

$$\delta_r \cdot f(r) \cdot r^{p_r}(t) \cdot f(b) \cdot b^{q_r}(t) \quad (10)$$

and analogously for the other kinetic interaction term in the equation system (8) avoids the occurrence of compartments with negative levels but preserves the system dynamics for  $b > 0$  approximately. For avoiding bulky expressions, we will use the designation  $\overline{x^a} := f(x)x^a$ . This simplifies term (10) to

$$\delta_r \cdot \overline{r^{p_r}(t)} \cdot \overline{b^{q_r}(t)}. \quad (11)$$

For simplifying the notation, the temporal derivative of e.g. a compartment level  $C(t)$  is designated as  $C'(t)$  in the future.

**Proposition 1** (Consistency of the Modified Equation System).

a) For  $b \rightarrow 0$  or  $r \rightarrow 0$  it holds  $\delta_r \cdot \overline{r^{p_r}(t)} \cdot \overline{b^{q_r}(t)} \rightarrow 0$  and

$$\delta_r \cdot \overline{r^{p_r}(t)} \cdot \overline{b^{q_r}(t)} \approx \delta_r \cdot r^{p_r}(t) \cdot b^{q_r}(t)$$

otherwise. An analogous statement is valid for the corresponding interaction term  $\delta_b \cdot \overline{b^{p_b}(t)} \cdot \overline{r^{q_b}(t)}$  for Red.

b)  $N_b \rightarrow 0 \Rightarrow N'_b(t), N'_r(t) \rightarrow 0$  and  $N_r \rightarrow 0 \Rightarrow N'_b(t), N'_r(t) \rightarrow 0$ .

*Sketch of Proof.*

a) According to the definition of the operator  $\overline{\phantom{x}}$ , it holds  $\overline{b^{q_r}(t)} \rightarrow 0$  for  $b \rightarrow 0$  and  $b^{q_r}(t) \approx \overline{b^{q_r}(t)}$  otherwise. In the first case, this is caused by  $f(b) \rightarrow 0$  for the additional factor  $f(b)$  occurring in  $\overline{b^{q_r}(t)}$ ; in the second case, this factor can be neglected due to  $f(b) \approx 1$ . A corresponding statement is valid for  $r^{p_r}(t)$ . The claim is an immediate consequence.

b) The condition  $N_b \rightarrow 0$  leads immediately to  $b \rightarrow 0$  due to the non-negativity of all force element type levels. Thus it holds  $\delta_b \cdot \overline{b^{p_b}(t)} \cdot \overline{r^{q_b}(t)} \rightarrow 0$  and  $\delta_r \cdot \overline{r^{p_r}(t)} \cdot \overline{b^{q_r}(t)} \rightarrow 0$ ; this results from part a). Since no other term can cause annihilation losses —  $\phi_{glj}$  and  $\alpha_{ikjgl}$  are just modifying the malware states of force elements — this gives  $N'_b(t), N'_r(t) \rightarrow 0$ , which is the claim. □

One has to note that a vanishing dynamics  $N'_b(t), N'_r(t) \rightarrow 0$  may not only be caused by a vanishing force size  $N_b$  or  $N_r$ , but also by vanishing kinetic effectiveness  $\delta_{b/r}$ .

If we speak about the equation system (8) in the following, we always mean the system modified by the barrier function  $f(x)$  as described above. The preceding proposition shows that the introduction of the barrier function  $f(x)$  excludes the two types of unphysical behavior mentioned at the beginning of this section. Such negativities can also be generated at the computational level due to overshooting effects, if the size of the time steps is not small enough. A less extreme barrier function  $f(x)$  — i.e. a barrier function with a smaller exponent — may avoid negativities more reliably, but its influence on the dynamics of the system will be stronger.

## 2.7 Model Properties

We derive several properties, which assure applicability and validity of the intended risk assessment procedure.

**Proposition 2** (Properties of the Equation System).

a) The equation system (8) is symmetric w.r.t. Blue and Red, i.e. an interchange of the initial conditions and parameters for Blue and Red corresponds to an interchange of the dynamics of the compartment levels  $b_{jl}(t)$ ,  $D_{b,j}(t)$  and  $r_{jl}(t)$ ,  $D_{r,j}(t)$ .

b) The quantities  $N_j(t) + D_j(t)$ ,  $j = 1, \dots, n$  and  $N(t) + D(t)$  are preserved over time. For an initial condition  $D_j(0) = 0$  resp.  $D(0) = 0$ , one gets  $N_j(0) = N_j(t) + D_j(t)$  resp.  $N(0) = N(t) + D(t)$  for all times  $t$ .

*Sketch of Proof.*

a) According to the structure of (8).

b) Combining (8) and the definition of  $D'_j(t)$  leads to  $N'_j(t) + D'_j(t) = 0$ , because all terms in the equation system cancel out. In this respect, one has to take the antisymmetry of  $\phi_{b/r,glj}$  and  $\alpha_{b/r,ikjgl}$  into account; since we sum up in  $N_j + D_j$  resp.  $N + D$  over both indices  $g, l$  of  $\phi_{glj}$  and  $\alpha_{ikjgl}$  subject to the antisymmetry constraint, it holds  $\sum_l \left( \sum_g \phi_{glj} \right) = 0$  and  $\sum_l \left( \sum_{ikg} \alpha_{ikjgl} \right) = 0$ . Thus,  $N_j(t) + D_j(t)$  is constant over time. The statements concerning  $N(t) + D(t)$  and  $N(0) = N(t) + D(t)$  are an immediate consequence. □

With help of proposition 2.b), the maximum possible annihilation losses are known. Another important aspect is the existence of a well-defined 'final' outcome. As soon as the simulation of the evolution of a given scenario has estimated the final outcome with sufficient accuracy, it may stop (see section 4.1). In reality, a battle does of course not necessarily stop with such final outcome, which usually corresponds to the annihilation of one of the forces. If a force is experiencing many losses when compared with the enemy, it might for example decide to break off combat and retreat. Since we are primarily interested in risk assessments and other evaluations and not in predictions of events to be expected, these additional options are considered as negligible. The definition of the final outcome is based on the following proposition.

**Proposition 3** (Dynamics at Infinity). It holds  $\lim_{t \rightarrow \infty} N_j'(t) = 0$  and  $\lim_{t \rightarrow \infty} D_j'(t) = 0$

*Sketch of Proof.* Due to the annihilation losses given by the terms  $\delta_{r,ikjl} \cdot r_{ik}^{p_{r,ikjl}}(t) \cdot b_{jl}^{q_{r,ikjl}}(t)$  and  $\delta_{b,ikjl} \cdot b_{ik}^{p_{b,ikjl}}(t) \cdot r_{jl}^{q_{b,ikjl}}(t)$  in the equation system (8),  $N_j(t)$  is monotonically decreasing. In this respect it is important to note that the other terms  $\phi_{glj}$  and  $\alpha_{ikjgl}$  in (8) are just modifying the malware states of force elements, but they do not change  $N_j(t)$ . According to  $N_j''(t) < 0$  — derivable directly from (8) — the decrease of  $N_j'(t)$  is monotonic as well; thus, an already small flow rate can not increase again. Due to the monotonic decrease of  $N_j(t)$  and  $N_j'(t)$  on the one hand and the limitation given by  $N_j(t) \geq 0$  on the other, the decrease must be fading out. This proves the claim  $N_j'(t) \rightarrow 0$ . The claim  $D_j'(t) \rightarrow 0$  follows immediately using proposition 2.b).  $\square$

### 3 Example: A Simple Homogeneous Model

#### 3.1 Setting of the Example

We give a simple example — continued in section 5 — how a specific kinetic-cyber situation can be represented in a model  $M \in \mathcal{M}$ . It serves for illustrative purposes and makes the idealistic assumption of homogeneous forces. This assumption may be approximatively fulfilled in situations like large tank battles or combat without heavy equipment [17, 18, 24, 29, 35]. As a consequence of the assumption of homogeneity, the dependence of  $\delta$ ,  $p$ , and  $q$  on the weapon system type is abandoned. For the Lanchester parameters  $p$  and  $q$ , a distinction of individual parameter values for Blue and Red is omitted. Accordingly, the equations (1) simplify to

$$\begin{aligned} b'(t) &= -\delta_r r^p(t) b^q(t) \\ r'(t) &= -\delta_b b^p(t) r^q(t) \end{aligned} \tag{12}$$

For the representation of the malware infection, we make use of the SIR-model given in (2). The basic model is slightly generalized by distinguishing between patching of infected and of vulnerable systems with rate  $\tilde{\gamma}$  and  $\gamma$ . Patching of infected systems requires an interaction with vulnerable or patched systems. Infected systems can not patch other systems or themselves. When coupling a homogeneous Lanchester model and a SIR model, the force elements have to be partitioned among the three different malware infection states —  $S$ ,  $I$ , and  $R$  — of the SIR model. These compartments were supplemented by the compartment  $D$  of destroyed force elements for bookkeeping purposes. As the result of the propagating malware, the kinetic effectiveness  $\delta$  of infected force elements is reduced by a factor  $\eta \in [0, 1]$ . The product  $\eta\delta$  can be interpreted as a modified kinetic effectiveness of attacking force elements infected with malware. It does not depend on the malware infection state of the force elements being attacked. This means that losses are suffered independently of their malware state, i.e. vulnerable, infected, and patched systems are affected according to the same attrition rate. The effectiveness is restored to its original value after patching. The option to distinguish between different values of  $p$ ,  $q$  in dependence of malware infection states is omitted.

#### 3.2 Model Structure

The setting of the example leads to the model structure in figure 1. We will now quantify the flows between the compartments belonging to the blue force; the flows for Red result from the

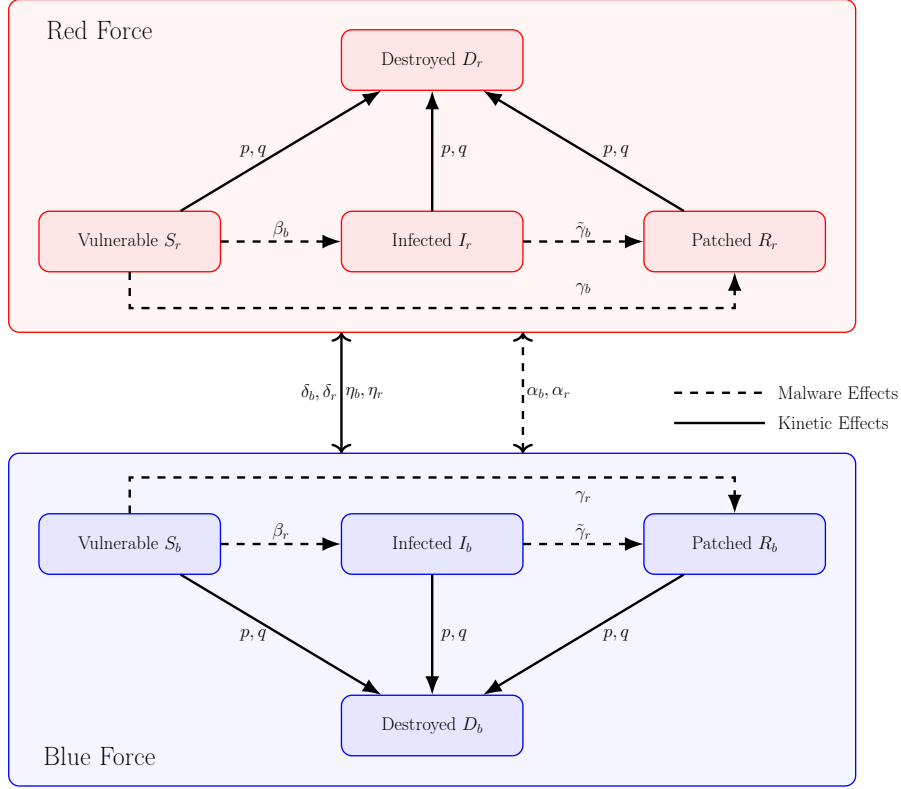


Figure 1: Red force and blue force fighting against each other on two levels: kinetic and cyber

intended symmetry of the model. We will use the designation  $N = S + I + R$  for the still existing force elements.

- $\beta_b S_b I_b / N_b$  is the flow from  $S_b$  to  $I_b$  representing the malware infection process.
- $\gamma_b S_b$  is the flow from  $S_b$  to  $R_b$  due to the patching of vulnerable (i.e. non-infected) elements.
- $\tilde{\gamma}_b I_b (S_b + R_b) / N_b$  is the flow from  $I_b$  to  $R_b$  representing a patch of the vulnerability for infected force elements. The removal of the malware infection is considered as part of the patching process.

Now, the flows related to kinetic combat are discussed. Following the structure of the equation system (12), the attrition rate of Red on Blue is  $\delta_r (S_r + R_r + \eta_r I_r)^p$ . The factor  $\eta_r$  in this term describes the reduced effectiveness of infected force elements. The affected elements of Blue are  $S^q$ ,  $I^q$ , or  $R^q$ .

- $\delta_r (S_r^p + R_r^p + \eta_r I_r^p) \cdot S_b^q$  is the flow from  $S_b$  to  $D_b$  due to kinetic combat losses.
- $\delta_r (S_r^p + R_r^p + \eta_r I_r^p) \cdot I_b^q$  is the flow from  $I_b$  to  $D_b$  due to kinetic combat losses.
- $\delta_r (S_r^p + R_r^p + \eta_r I_r^p) \cdot R_b^q$  is the flow from  $R_b$  to  $D_b$  due to kinetic combat losses.
- $\alpha_r (S_r + R_r) \cdot S_b$  is the flow from  $S_b$  to  $I_b$  due to a malware attack of Red. It should be noted, that  $\alpha$  is here used as a scalar coefficient instead of a flow function as in (8).

In the end, we get four equations for each of the two forces. We only give the equations for Blue, since the equations for Red have symmetric form. Additional remarks about the basic structure



of such an equation systems can be found in [47, 60].

$$\begin{aligned}
S'_b(t) &= -\beta_b S_b I_b / N_b - \gamma_b S_b \\
&\quad - \delta_r (S_r^p + R_r^p + \eta_r I_r^p) \cdot S_b^q \\
&\quad - \alpha_r (S_r + R_r) \cdot S_b \\
I'_b(t) &= \beta_b S_b I_b / N_b - \tilde{\gamma}_b I_b (S_b + R_b) / N_b \\
&\quad - \delta_r (S_r^p + R_r^p + \eta_r I_r^p) \cdot I_b^q \\
&\quad + \alpha_r (S_r + R_r) \cdot S_b \\
R'_b(t) &= \gamma_b S_b + \tilde{\gamma}_b I_b (S_b + R_b) / N_b \\
&\quad - \delta_r (S_r^p + R_r^p + \eta_r I_r^p) \cdot R_b^q \\
D'_b(t) &= \delta_r (S_r^p + R_r^p + \eta_r I_r^p) \cdot (S_b^q + I_b^q + R_b^q)
\end{aligned} \tag{13}$$

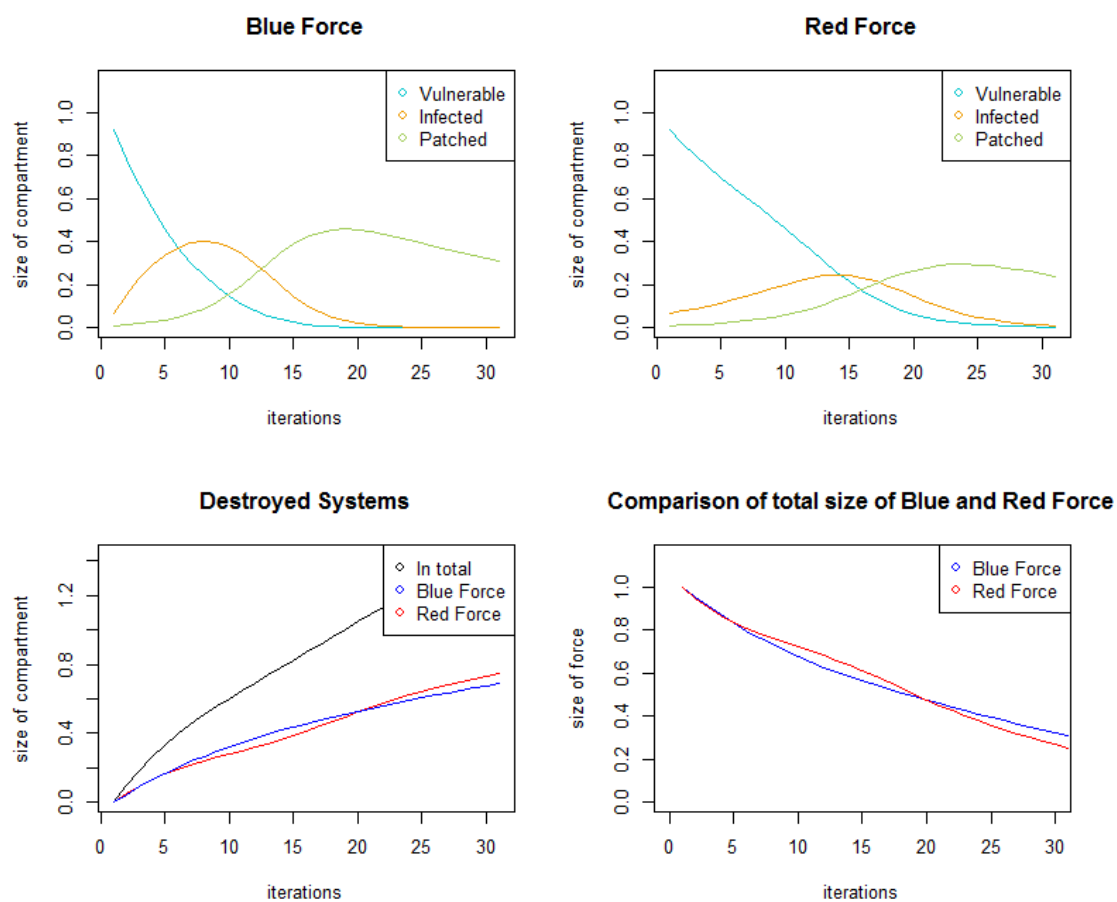


Figure 2: A typical behavior of the equation system (13). Besides of the number of vulnerable, infected, and patched elements for both forces, the overall numbers of available and destroyed force elements are shown. Due to malware attacks applied by both forces, the red force is stronger at the beginning but will still lose in the end.

### 3.3 Model Parameters

Model parameters are listed in table 1. Except of  $p, q$ , the given parameters can be chosen independently for Blue and Red. As initial conditions, the non-negativity  $S(0), I(0), R(0), D(0) \geq 0$  of all compartments is required. Compared to the models of Schramm [47] and Yildiz [60],

Parameter Group	Parameter with Description	Parameter Range
<b>Kinetic Combat</b>	$\delta$ Kinetic effectiveness of vulnerable and patched elements	$\delta \geq 0$
	$\eta$ Effectiveness reduction of infected elements	$\eta \in [0, 1]$
	$p$ First Lanchester parameter	$p \geq 0$
	$q$ Second Lanchester parameter	$q \geq 0$
<b>Cyber Combat</b>	$\alpha$ Malware attack rate	$\alpha \geq 0$
<b>Malware Spreading</b>	$\beta$ Infection rate	$\beta \geq 0$
	$\gamma$ Patch rate for vulnerable elements	$\gamma \in [0, 1]$
	$\tilde{\gamma}$ Patch rate for infected elements	$\tilde{\gamma} \in [0, 1]$
<b>Timing</b>	$\Delta t_{\text{att}}$ Time difference $\Delta t_{\text{att}} = t_{\text{att}} - t_{\text{kin}}$ between the start $t_{\text{att}}$ of the malware attack and the start $t_{\text{kin}}$ of kinetic combat.	$\Delta t_{\text{att}} \in \mathbb{R}$
	$\Delta t_{\text{mal}}$ Duration of malware attack	$\Delta t_{\text{mal}} \geq 0$
	$\Delta t_{\text{pat}}$ Time difference $\Delta t_{\text{pat}} = t_{\text{pat}} - t_{\text{kin}}$ between the start $t_{\text{pat}}$ of the patching process (for both vulnerable and infected elements) and the start $t_{\text{kin}}$ of the kinetic combat	$\Delta t_{\text{pat}} \in \mathbb{R}$

Table 1: Parameters occurring in the equation system (13).

the example introduces some generalizations. The generalization of the Lanchester exponents  $p, q$  from  $p = 1, q = 1$  as in [47, 60, 61] to  $p, q \in \mathbb{R}_0^+$  gives a significantly improved description of many historic battles [17, 35]. Concerning the SIR component, we distinguish the patching rates  $\gamma, \tilde{\gamma}$  of vulnerable and already infected force elements, because we assume that the removal of a malware infection takes additional time. Furthermore, the intensity of the malware attack is parameterized by  $\alpha$ .

Table 1 includes event time parameters, which extend the model by allowing an onset of kinetic combat, malware attack and patching process independent from each other. In this way, situations like a preparation of a kinetic battle by a supporting malware attack in advance or a late start of countermeasures due to a delayed provision of appropriate patches can be modeled. Usually, the force under malware attack will also need some time to recognize the attack and to initiate corresponding countermeasures. Additionally, the duration of the malware attack can be determined by  $\Delta t_{\text{mal}}$ . An early stop of the malware attack can sometimes be useful for covering up the source of the malware attack.

Before the start and after the end of an action like malware attack, the execution of the action is inhibited by appropriate parameter settings. In between, the action is activated by setting its parameters to their effective values. Details of the translation of the timing parameters given in table 1 to corresponding event-based changes of the parameter settings are given in table 2. Figure 3 depicts events and time intervals used in the text graphically.

Events	Associated Parameter Changes
Initial settings	$\alpha, \delta, \gamma, \tilde{\gamma} = 0$
Start of kinetic combat at time $t_{\text{kin}}$	$\delta$ set to (effective) parameter value
Start of malware attack at time $t_{\text{att}} = t_{\text{kin}} + \Delta t_{\text{att}}$	$\alpha$ set to (effective) parameter value
Stop of malware attack at time $t_{\text{att}} + \Delta t_{\text{mal}}$	$\alpha = 0$
Start of patching process at time $t_{\text{pat}} = t_{\text{kin}} + \Delta t_{\text{pat}}$	$\gamma, \tilde{\gamma}$ set to (effective) parameter values

Table 2: Translation of the events associated with the timing parameters given in table 1 to corresponding changes of the parameter settings.

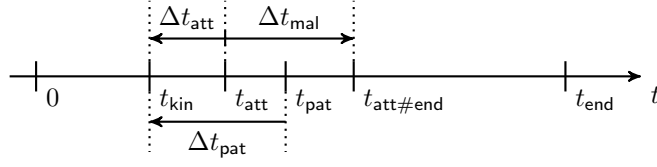


Figure 3: Designations of events and time intervals as used in the text.

### 3.4 Model Validation

For demonstrating the validity of the model (13), we have to show that the model behavior is sufficiently similar to the real system. Unfortunately, corresponding real-world data sets are missing or at least not accessible to the public. We thus show the validity of the two main components of the overall model by applying a cross-validation with basic models of the pure Lanchester and SIR equations. An explicit validation of the main components of the overall model seems to be necessary; despite of the already provided arguments supporting the validity of the two main components when being considered in isolation, additional modes of dynamics may occur in the integrated system (13) compared to isolated Lanchester or SIR models. This validation strategy is applicable to more general heterogeneous Lanchester models and extensions of SIR models as well. After showing the validity of the two main components, the interactions between them have to be considered in a validation task of its own. Details of the three validation steps are given in the following.

*Validation of the Lanchester Component:* Concerning the Lanchester part of (13), the authors refer to [17, 18, 24, 29, 35] regarding the usability of the Lanchester model as basic reference model. For executing the comparison, all model parameters are set to zero resp. neutral values with exception of  $\delta_b, \delta_r, p, q$ . With respect to the effectiveness reduction of force elements due to malware infections, the values  $\eta_b, \eta_r = 1$  have been chosen.

*Validation of the SIR Component:* Concerning the SIR-model as a description of a malware epidemic, see [47] and the references therein. The realism of compartmental models for representing a malware epidemics is supported in [12]. The cross-validation uses the model parameters  $\beta, \gamma, \tilde{\gamma}$ . Other parts of the model (13) are switched off by  $\delta_b, \delta_r, \alpha_b, \alpha_r = 0$ . This leads to the following comparison model.

$$\begin{aligned}
 S'_b(t) &= -\beta_b S_b I_b / N_b - \gamma_b S_b \\
 I'_b(t) &= \beta_b S_b I_b / N_b - \tilde{\gamma}_b I_b (S_b + R_b) / N_b \\
 R'_b(t) &= \gamma_b S_b + \tilde{\gamma}_b I_b (S_b + R_b) / N_b
 \end{aligned} \tag{14}$$

This equation system differs from common SIR-models with biological origin by an unusual 'recovery' term  $\tilde{\gamma}_b I_b (S_b + R_b) / N_b$ . For the cross-validation, we have chosen the initial conditions  $S_b(0) \in [0.1, 1.0]$  and  $I_b(0) := 0.1 \cdot S_b$ . Since the parameter settings for the cross-validation switch off malware attacks, we have to start with a non-zero fraction of infections.

*Validation of the Component Interactions:* Our validation approach concerning the interactions between the Lanchester and the SIR component relies on confidence building. For this purpose, plausibility arguments are checked. This includes the reproduction of essential behavioral characteristics. The checked properties encompass, that a larger force cannot give a worse outcome under — apart from that — equal conditions, that a larger kinetic effectiveness of one side increases the losses of the other side and that a combined kinetic-cyber attack cannot give a worse outcome than a pure kinetic attack. Beyond that, the reproducibility of model properties formally derived from (13) like the conservation of the numbers  $N_b(t) + D_b(t)$ ,  $N_r(t) + D_r(t)$  of force elements and the monotonic decrease of existing force elements  $N_b(t)$ ,  $N_r(t)$  over time were examined. Other such properties are provided in [47, 60].

## 4 Simulation-based Risk Assessment

### 4.1 Simulation Trajectories

In order to assess the risk inherent to a scenario  $x \in X$ , the outcome of the situation represented by  $x$  is determined based on the equation system (8) [14, 15]. For this purpose, a standard differential equation solver of computational mathematics is applied, which approximates the time-dependent solution of the differential equation by taking finite discrete steps  $h$  on the time-axis. For being well-defined, the error inherently involved in such an approximation must vanish for  $h \rightarrow 0$ . This property is assured by Lipschitz continuity, which is shown in the following proposition.

**Proposition 4** (Lipschitz continuity). The equation system (8) is Lipschitz continuous.

*Proof.* Proposition 2.b) assures the conservation of the overall numbers  $N_j(t) + D_j(t)$  of both blue and red elements over time. Due to  $N_j(t), D_j(t) \geq 0$ , the numbers  $N_j(t), D_j(t)$  are thus bounded from above. This also holds for the stock levels  $b_{jl}(t), r_{jl}(t)$  comprising  $N_j(t)$ . Since we have assured that all flow terms  $\phi_{glj}$  remains bounded (see page 4), the expressions for the derivatives in equation system (8) remain bounded as well. Lipschitz continuity of the equation system (8) is an immediate consequence.  $\square$

The space  $X$  of scenarios is the Cartesian product of the domains of the input parameters and of the initial values. It is also called *design space*. Executing the simulation  $\text{sim}: X \rightarrow Y$  assigns an outcome  $y \in Y$  to the input  $x \in X$ . The space  $Y = \mathbb{R}_0^+ \rightarrow (\mathbb{R}_0^+)^{4n}$  of simulation outcomes records the dynamics of the model (8) as the time-dependent variations of the force element numbers. Thus, an outcome  $y \in Y$  consists of  $N_j(t), D_j(t)$  for both Blue and Red with  $t \in T = [0, \infty[$  as the simulation time. Since for function spaces usually no *canonical* ordering ' $<$ ' exists, it is reasonable to ask how outcomes can be compared with each other. Proposition 3 improves the situation, because it shows that the annihilation dynamics in equation system (8) is fading out for  $t \rightarrow \infty$ . This justifies to identify an outcome with the values  $\lim_{t \rightarrow \infty} N_j(t), \lim_{t \rightarrow \infty} D_j(t)$  of its constituents in the far future for both Blue and Red. Since these values are real numbers, a canonical ordering ' $<$ ' is available for comparison purposes then.

The fading dynamics may also be used to trigger a stop of the simulation, if

$$|N_j(t) - N_j(t + \Delta\tau)| < \varepsilon \text{ for all } j \quad (15)$$

holds for a 'long' time period  $\Delta\tau$ . The end time of the simulation given by the stopping criterion is designated as  $t_{\text{end}}$ . Since special events like a malware attack may modify parameter values and thus change the considered situation in a fundamental way, we have to assure that no such event has still to be processed when a stop of the simulation run is declared. In the example of section 3, we thus start to check criterion (15) only for  $t > t_{\text{kin}}, t > t_{\text{att}} + \Delta t_{\text{mal}}$ , and  $t > t_{\text{pat}}$  simultaneously. In order to work properly,  $\Delta\tau$  has to be chosen sufficiently large and  $\varepsilon$  sufficiently small. Unfortunately, for each choice of  $\Delta\tau$  and of  $\varepsilon$  there exist scenarios with an arbitrary slow dynamics leading to large approximation errors. For them, the simulation stops early providing intermediate instead of 'final' results. These exceptions are tolerable, as long as they are so rare that the outcome statistics remains unaffected.

In the following proposition, we state that an almost vanished force will not change its own size significantly anymore and will also be unable to change the size of the opposing force significantly because of its almost vanished fighting power. The proposition is a generalization of proposition 1.b).

**Proposition 5** (Effects of a Destroyed Force). If  $N_r \rightarrow 0$  or if  $N_b \rightarrow 0$ , then  $N'_b, N'_r, D'_b, D'_r \rightarrow 0$ .

*Proof.* W.l.o.g one can assume  $N_b(t) \rightarrow 0$ ; otherwise exchange blue and red side. The claim  $N_b(t) \rightarrow 0 \Rightarrow N'_b(t), N'_r(t) \rightarrow 0$  holds according to proposition 1.b). Proposition 2.b) states that  $N_r(t) + D_r(t)$  is constant over time; thus,  $N'_{b/r}(t) \rightarrow 0$  gives  $D'_{b/r}(t) \rightarrow 0$  as well.  $\square$

The application of the criterion for triggering the stop of the simulation leads to the simulation algorithm 1.

---

**Algorithm 1** Simulation Algorithm
 

---

```

1: procedure SIMULATION
2:   loop
3:     Calculate system state for new time step  $t$ 
4:     exit if  $\forall j: |N_j(t) - N_j(t + \Delta\tau)| < \varepsilon \wedge |D_j(t) - D_j(t + \Delta\tau)| < \varepsilon$ 
5:      $t \leftarrow t + \delta t$  ▷ Transition to next Euler step
6:   end loop
7:    $t_{\text{end}} \leftarrow t$  ▷ End time of simulation
8: end procedure

```

---

## 4.2 Observables

Survivors  $N_b(t), N_r(t)$  and losses  $D_b(t), D_r(t)$  are recording the effects of a malware infection. Since  $N_b(t), N_r(t)$  are non-negative, the relative number  $\Delta N := N_b(t_{\text{end}}) - N_r(t_{\text{end}})$  of surviving force elements can be used as an assessment criterion of the final outcome. Analogously, the relative number  $\Delta D := D_b(t_{\text{end}}) - D_r(t_{\text{end}})$  of destroyed elements can be applied. If interested in absolute numbers, the cumulative losses  $L_b := D_b(t_{\text{end}})$  of the blue force may be preferred. A list of the observables used in this paper are given in table 3. Hereafter, the set of values of an observable, say,  $\Delta N$ , for a set  $\tilde{X} \subseteq X$  of scenarios is designated as  $\Delta N(\tilde{X})$ . Analogously, the set of values of an input parameter, say,  $\alpha_b$  occurring in  $\tilde{X}$  is designated as  $\alpha_b(\tilde{X})$ .

The interpretation of the relative assessment criteria  $\Delta N$  and  $\Delta D$  is straightforward. The case  $\Delta N > 0$  indicates a win of Blue, whereas the case  $\Delta N < 0$  indicates a win of Red. A situation with  $\Delta N = 0$  could be judged as a draw. Analogously,  $\Delta D > 0$  indicates an advantage for Red concerning the involved risks, whereas  $\Delta D < 0$  indicates an advantage for Blue. Again,  $\Delta D = 0$  could be judged as a draw because the losses of both sides have the same amount. The inclusion of both  $\Delta N$  and  $\Delta D$  is justified, because results with e.g.  $\Delta N > 0$  and  $\Delta D > 0$  are possible due to different force sizes and force effectivenesses.

**Definition** (Wins and Losses). Based on the relative assessment criteria  $\Delta N$  and  $\Delta D$ , we provide the following definitions of wins and losses, given from the perspective of Blue.

Defined Notion (for Blue)	Condition on $\Delta N$	Condition on $\Delta D$
Strong win	$\Delta N > 0$	$\Delta D < 0$
Weak win	$\Delta N > 0$	$\Delta D > 0$
Weak loss	$\Delta N < 0$	$\Delta D < 0$
Strong loss	$\Delta N < 0$	$\Delta D > 0$

We supplement the above notions with corresponding definitions at the pure kinetic level. This will allow us to quantify the influence of a malware epidemic by e.g. measuring the fraction of situations, in which cyber warfare gives an advantage despite of losing a pure kinetic battle.

**Definition** (Kinetic Superiority and Kinetic Inferiority). Let  $g_{\text{kin}}: X \rightarrow X; x \mapsto x'$  designate a mapping between scenarios, which set the kinetic effectiveness  $\delta$  of the force elements to values assigned to force elements, which are not infected by malware. Thus,  $\delta$  becomes independent on the malware infection states of attacker and defender. All other model parameter settings are left unchanged. The mapping  $g_{\text{kin}}$  provides a pure kinetic scenario  $x'$  resulting from  $x$  by hiding all malware effects. With respect to  $x'$ , we give the following definitions.

Defined Notion (for Blue)	Condition on $\Delta N$	Condition on $\Delta D$
Strong kinetic superiority	$(\Delta N) \circ g_{\text{kin}} > 0$	$(\Delta D) \circ g_{\text{kin}} < 0$
Weak kinetic superiority	$(\Delta N) \circ g_{\text{kin}} > 0$	$(\Delta D) \circ g_{\text{kin}} > 0$
Weak kinetic inferiority	$(\Delta N) \circ g_{\text{kin}} < 0$	$(\Delta D) \circ g_{\text{kin}} < 0$
Strong kinetic inferiority	$(\Delta N) \circ g_{\text{kin}} < 0$	$(\Delta D) \circ g_{\text{kin}} > 0$

**Proposition 6** (Extrema of Observables). Let us assume  $D_b(0), D_r(0) = 0$ .

- a) It holds  $\max(\Delta N) = \max(\Delta D) = N_b(0)$  and  $\min(\Delta N) = \min(\Delta D) = -N_r(0)$ .
- b) It holds  $\max(L_b) = N_b(0)$  and  $\min(L_b) = 0$ .

*Sketch of Proof.*

- a) Due to the definition of  $\Delta N$  and the monotonic decrease of  $N_b$ , the observable  $\Delta N$  can not have a value larger than  $N_b(0)$ . At the end of the simulation, it reaches this value if all force elements of Blue survive e.g. due to  $\delta_{r,ijkl} = 0$  and if no elements of Red survive due to  $\delta_{b,ijkl} > 0$ . Proposition 2.a) leads to  $\min(\Delta N) = -N_r(0)$ . The corresponding statements for  $\Delta D$  are a consequence of the preservation of  $N(t) + D(t)$  over time according to proposition 2.b).
- b) Proof analogous to a)

□

Quantitative assessments enable comparisons of scenario outcomes. For additionally being able to judge a *single* outcome as especially 'good' or 'bad', the ranges of possible assessment values have to be known. They are provided by Proposition 6.

### 4.3 Sampling of Simulation Outcomes

The details of a future (or current) malware attack may not be known exhaustively. In such a case, the scenario to be considered in the risk assessment process will not be uniquely determined. The existing uncertainties have to be included in the approach. The usually infinite size of the scenario space  $X$  compatible with the existing uncertainties rules out a brute-force processing. Instead, a small randomly selected subset  $\tilde{X} \subset^{\text{fin}} X$  of scenarios is analyzed. This leads to a Monte-Carlo approach for calculating the risk with inclusion of uncertainties approximatively. In the following, the subset  $\tilde{X}$  is called the *simulation design*. The set of outcomes of the simulation scenarios  $\tilde{X}$  is designated as  $\tilde{Y} \subseteq Y$ .

In order to enable the intended random selection, the scenario space  $X$  is enriched by a notion of probability. This gives the so-called *Monte-Carlo design space*  $(X, \text{Prob})$ . For assuring the appropriateness of the random sample  $\tilde{X}$ , the probability distribution  $\text{Prob}$  has to encode the frequency of occurrence of the different scenarios  $x \in X$ . In this way, the probability distribution  $\text{Prob}$  represents the knowledge about the considered situation.

The encoding of available and missing knowledge to a corresponding probability distribution  $\text{Prob}$  follows information-theoretic principles. We have to avoid that  $\text{Prob}$  contains more information about the situation than actually given; consequently, we choose the probability distribution  $\text{Prob}$  with the highest entropy among all distributions compatible with the given information. According to [28], the entropy  $H(\text{Prob})$  of a continuous probability distribution  $\text{Prob}$  is given by  $H(\text{Prob}) = - \int \text{Prob}(x) \log \text{Prob}(x) dx$ .

If the initially available knowledge is minimal in the sense of information-theory, only a lower and an upper limit of the domain of support is given. Renouncing any knowledge would be a problem, because in this case the finiteness of the entropy  $H(\text{Prob})$  can not be assured anymore. The resulting uniform distribution [7] (see table 4) may raise some scepticism, because uniformly distributed parameters are not justified by observations. We have to take care when interpreting the role of the uniform distribution, however. The uniform probability distribution of the input parameters does not represent a single specific situation, but a kind of 'superposition' of the variety of all *possible* distributions compatible with the available knowledge. Table 4 gives some

Observables	Description	Codomain
$\Delta N := N_b(t_{\text{end}}) - N_r(t_{\text{end}})$	Relative number of existing force elements at $t_{\text{end}}$	$\Delta N \in \mathbb{R}$
$\Delta D := D_b(t_{\text{end}}) - D_r(t_{\text{end}})$	Relative number of destroyed elements at $t_{\text{end}}$	$\Delta D \in \mathbb{R}$
$L_b := D_b(t_{\text{end}})$	Destroyed elements of the blue force at $t_{\text{end}}$	$L_b \in \mathbb{R}_0^+$

Table 3: List of the observables used for assessment purposes.

maximum entropy probability distributions for different kinds of basic knowledge. We restrict ourselves to distributions used in the example presented in section 5. Concerning parameters with a finite support, the uniform distribution is used if no further knowledge is available. If additionally expected values are known, the Beta distribution results. For a support equal to  $\mathbb{R}_+^0$ , the exponential distribution results in the case of a known expected value. Additional knowledge of the standard deviation leads to a lognormal distribution. In the case of a support equal to  $\mathbb{R}$ , the normal distribution has to be selected for known expected value and standard deviation.

Type	Support	Constraints	Probability Density
Uniform	$[a, b]$		$f(x) = \frac{1}{b-a}$ with $a \neq b$
Exponential	$[0, \infty)$	$E(x) = 1/\lambda$	$f(x) = \lambda \exp(-\lambda x)$
Normal	$(-\infty, \infty)$	$E(x) = \mu, \text{Var}(x) = \sigma^2$	$f(x) = \frac{1}{\sigma\sqrt{2\pi}} \exp\left(-\frac{1}{2}\left(\frac{x-\mu}{\sigma}\right)^2\right)$
Beta	$[a, b]$	$E(x) = \frac{\alpha \cdot b + \beta \cdot a}{\alpha + \beta}$ $E(b-x) = \frac{\beta \cdot b + \alpha \cdot a}{\alpha + \beta}$	with $a \neq b, f(x) =$ $\frac{1}{(b-a)B(\alpha, \beta)} \left(\frac{x-a}{b-a}\right)^{\alpha-1} \left(\frac{b-x}{b-a}\right)^{\beta-1}$
Lognormal	$[0, \infty)$	$E(\ln(x)) = \mu$ $E((\ln(x) - \mu)^2) = \sigma^2$	$f(x) = \frac{1}{\sigma x \sqrt{2\pi}} \exp\left(-\frac{(\ln(x) - \mu)^2}{2\sigma^2}\right)$

Table 4: Maximum entropy probability distributions resulting from basic constraints according to [43]. In the table,  $B$  designates the Beta function.

The inclusion of the knowledge resp. uncertainty perspective gives the following picture. Input parameters of the model subject to uncertainties may vary, taking on different values. Their variation is described by the probability distribution  $\text{Prob}$  of the space  $(X, \text{Prob})$ . Thus we can state, that in the presented approach fixed parameter values may be replaced by fixed probability distributions characterizing their variations. The accompanying transition from a point estimate to a statistics of estimates gives a richer description of the model behavior.

Though a random selection of the scenarios successfully avoids a selection bias, it may introduce a possible statistical bias. For monitoring the statistical quality, we compare the measured properties of the sampled subset  $\tilde{X} \subset X$  with the exact properties of the full design  $(X, \text{Prob})$ . The outcomes  $\tilde{Y}$  can be used for monitoring purposes as well. Numerical results of such comparisons are shown in figure 4.

#### 4.4 Risk Assessment by Sampling

Uncertainties of the input parameters may especially cause a variation of the losses  $L = D(t_{\text{end}})$ . This leads to the notion of risk in a straightforward way.

**Definition (Risk).** The *risk*  $\mathcal{R}$  assigned to a scenario  $x \in X$  is defined as  $\mathcal{R} := L(x)$ . If due to epistemic uncertainties a set of scenarios has to be considered given by the Monte-Carlo design  $(\tilde{X}, \text{Prob})$ , the risk  $\mathcal{R}$  is more generally defined as expected value  $\text{mean}(L(\tilde{X}))$ .

From a computational perspective, the risk may be determined approximatively as the mean loss of the random sample of scenarios in accordance with [3]. In the following proposition, some properties of risk are derived.

**Proposition 7 (Properties of Risk).** Let a simulation design  $\tilde{X}$  be given. We assume  $D(0) = 0$ .

- It holds  $\text{mean}(N(0)) = \text{mean}(N(t_{\text{end}})) + \text{mean}(D(t_{\text{end}})) = \text{mean}(N(t_{\text{end}})) + \mathcal{R}$
- $\mathcal{R} \leq \max(N(0))$ .

*Proof.*

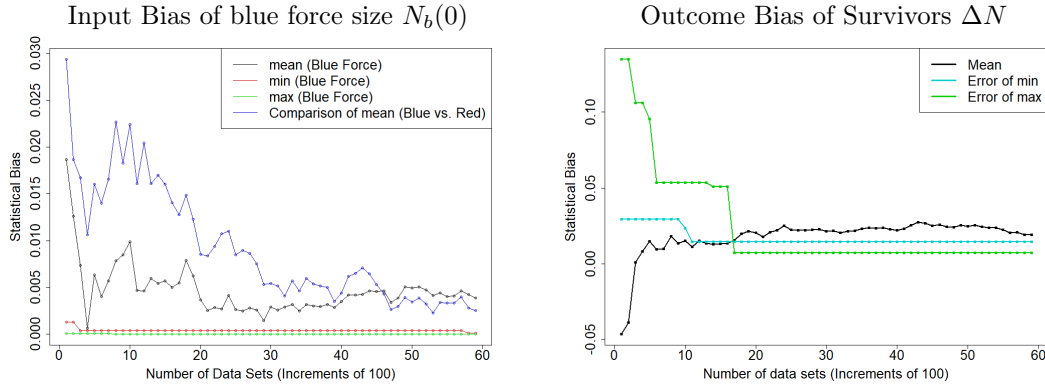


Figure 4: Statistical bias of random sampling dependent on the number of simulation runs. The comparison of statistical quantities of the simulation design  $\tilde{X}$  (and of the associated outcomes  $\tilde{Y}$ ) with theoretical predictions for the corresponding full design allows a monitoring of the statistical bias. If the bias turns out to be too high, the size of the simulation design has to be increased accordingly.

As an example, we consider uniformly distributed force sizes  $N_b(0), N_r(0) \in [0, 1]$  (left) and the resulting behavior of  $\Delta(N)$  (right) in a symmetric situation. Let us write  $\tilde{N} := N_b(0)$  for short. Concerning the input, the plot includes the difference between the measured value  $\text{mean}(\tilde{N}(\tilde{X}))$  and the theoretically expected value 0.5, analogously the deviation of  $\text{min}(\tilde{N}(\tilde{X}))$  resp.  $\text{max}(\tilde{N}(\tilde{X}))$  from 0 resp. 1, and finally the difference of  $\text{mean}(\tilde{N}(\tilde{X}))$  between Blue and Red. Concerning the outcome, the plot includes  $\text{mean}(\Delta N(\tilde{X}))$  and the deviation of  $\text{max}(\Delta N(\tilde{X}))$  resp.  $\text{min}(\Delta N(\tilde{X}))$  from 1.0 resp.  $-1.0$  as given by proposition 6.a). All considered input and outcome quantities will have the value zero for a completely bias-free statistics.

- a) According to proposition 2.b), one gets  $N(0) = N(t_{\text{end}}) + D(t_{\text{end}})$ . Applying the operator mean and taking its linearity into account, the definition of  $\mathcal{R}$  gives the claim.
- b) According to the proof of part a), it holds  $\text{mean}(N(0)) = \text{mean}(N(t_{\text{end}})) + \mathcal{R}$  and thus  $\text{max}(N(0)) \geq \text{mean}(N(0)) \geq \mathcal{R}$ .

□

## 5 Example: Analyzing Homogeneous Lanchester-SIR

### 5.1 A Sequence of Situations with Decreasing Uncertainty

Parameter	Situational Description	Constraints
Initial size of forces $N_b, N_r$	The scale of forces involved in combat is unknown. We only assume a plausible lower and upper limit.	Finite support, $N(0) \in [0.1, 1]$
Kinetic effectiveness $\delta_b, \delta_r$	Expected values of kinetic effectiveness exist, but the available data do not suffice for providing the standard deviation.	$E(\delta) = 1.2$ for Blue and Red
Lanchester parameters $p, q$	As for the kinetic effectiveness, expected values exist, but not standard deviations. The probability distributions of $p$ and $q$ coincide, because we do not know which force is attacking and which defending.	$E(p) = E(q) = 2.5$

Table 5: Initial uncertainty constraints on the kinetic parameters of the example.

The evaluation approach is applied to the Lanchester-SIR model introduced in section 3. Initially, we consider a situation without specific conflict ahead. Technological breakthroughs, economic



Parameter	Situational Description	Constraints
Time difference $\Delta t_{\text{att}}$ between kinetic and cyber attack	The start times of malware attack and kinetic combat will not differ substantially. A late start is uncommon due to the limited influence on kinetic combat. An early start, on the other hand, gives the opponent time to develop a patch.	$E(\Delta t_{\text{att}}) = 0$ , $\text{Var}(\Delta t_{\text{att}}) = 25^2$
Duration $\Delta t_{\text{mal}}$ of malware attack	We only assume a plausible lower and upper bound.	Finite support, $\Delta t_{\text{mal}} \in [0.1, 10]$
Malware attack rate $\alpha$	We assume a plausible upper bound.	Finite support, $\alpha \in [0, 1]$
Initial number $R(0)$ of non-vulnerable force elements	Blue uses a large variety of software systems, which lowers the probability that a malware epidemics covers a large fraction of its force. It holds $I(0) = 0$ and thus $S(0) = N(0) - R(0)$ .	We assume $E(R_b(0)) = 5N_b(0)/7$ , $E(S_b(0)) = 2N_b(0)/7$ , $E(R_r(0)) = N_r(0)/2$ , $E(S_r(0)) = N_r(0)/2$
Infection rate $\beta$	Experience may provide the expected infection rate and its standard deviation.	$E(\ln(\beta)) = \mu = 1$ and $E((\ln(\beta) - \mu)^2) = \sigma^2 = 1$
Effectiveness reduction $\eta$ of infected elements	The support of $\eta \in [0, 1]$ is given by definition. Experience gives expected values as a supplement.	Finite support $\eta \in [0, 1]$ with $E(\eta) = 0.5$ and $E(1 - \eta) = 0.5$

Table 6: Initial uncertainty constraints on the cyber attack parameters of the example.

Parameter	Situational Description	Constraints
Time difference $\Delta t_{\text{pat}}$ between patching and kinetic attack	Again, we assume a start time $\Delta t_{\text{pat}}$ of patching close to the start of kinetic combat. Patching will have no influence when applied after kinetic combat. Patching early then again usually just leads to the exploit of another vulnerability than the already patched one.	$E(\Delta t_{\text{pat}}) = 0$ , $\text{Var}(\Delta t_{\text{pat}}) = 25^2$
Patch rate $\gamma$ for vulnerable elements	As for the infection rate, we can provide expected values based on previous experience. The value for Blue and Red differ.	We assume $E(\gamma_b) = 1/4$ , $E(1 - \gamma_b) = 3/4$ , $E(\gamma_r) = 1/6$ , $E(1 - \gamma_r) = 5/6$
Patch rate $\tilde{\gamma}$ for infected elements	Again, we can provide expected values based on previous experience. We adopt a smaller patch rate for infected elements than for vulnerable elements, i.e. $0 \leq \tilde{\gamma} \leq \gamma$ .	We assume $E(\tilde{\gamma}_b) = \gamma_b/2$ , $E(\gamma_b - \tilde{\gamma}_b) = \gamma_b/2$ , $E(\tilde{\gamma}_r) = \gamma_r/2$ , $E(\gamma_r - \tilde{\gamma}_r) = \gamma_r/2$

Table 7: Initial uncertainty constraints on the cyber patching parameters of the example.

collapse, and other unforeseen events may lead to an large variety of future scenarios. The resulting uncertainties are given in the tables 5, 6, and 7. Over time, these uncertainties about the expected combat situation may be eliminated stepwise due to an increasing amount of knowledge and the decisions that have been made. This leads to a sequence of decreasing uncertainty. The corresponding sequence of risk assessments is given in section 5.2. In this exemplary course of action, the analysis results sometimes influence the hypothetical decisions.

The considerations contain some simplifications. First, the start times  $\Delta t_{\text{att}}$ ,  $\Delta t_{\text{pat}}$  and other parameters of cyber actions result in practice from control decisions. These are not part of the model and replaced by random parameter settings (see section 5.5). This is justified by the fact, that watching out for vulnerabilities and patching them is a continuously executed

process. Accordingly, patching is not necessarily a consequence of a malware attack. Exploiting information provided by intelligence can foil the principal causal order between malware attack and patching action as well. Furthermore, just intending to develop malware with a given infection rate or to close a vulnerability with a required patch rate does not mean that such a project can indeed be realized due to possible technical limitations and organizational frictions. Second, the uncertainties of the model parameters are assumed to be essentially independent from each other. The authors have made several exceptions, however, which are indicated in the tables 5, 6, and 7. Now, we present the uncertainty sequence going to be examined.

**Step 1 (Start Situation):** The parameters are uncertain at the beginning, because the circumstances of the next conflict are unknown (see tables 5, 6, 7).

**Step 2 (Force Selection):** A conflict emerges with a foreign state. An expeditionary force is sent. Accordingly, the opposing kinetic forces are known and the values of the uncertain parameters given in table 5 can be fixed for Blue and Red. The new knowledge consists of  $N_b(0) = 0.15$ ,  $N_r(0) = 0.3$ ,  $\delta_b = 2.0$ ,  $\delta_r = 0.8$ ,  $p = 2.5$ ,  $q = 1.7$ .

**Step 3 (Cyber Attack):** Since the enemy turns out to be superior from the kinetic perspective, a cyber attack concurrent to kinetic combat is planned. Here, own superiority was assumed from the beginning (see table 6), but with large uncertainties due to intelligence gaps. Accordingly, the cyber part of Red is a focus of blue intelligence. As a result, the cyber attack parameters of table 6 can be determined for Blue. Force elements, which cannot be infected by the malware in principle, are represented by an initial number  $R(0) \geq 0$ . The blue cyber attack is characterized by the parameters settings  $\Delta t_{b,\text{att}} = -15.0$ ,  $\Delta t_{b,\text{mal}} = 1.0$ ,  $\alpha_b = 0.5$ . The effect of the malware attack on Red is described by  $R_r(0) = 0.15$ ,  $S_r(0) = 0.15$ ,  $\beta_r = 1.75$ ,  $\eta_r = 0.15$ .

**Step 4 (Enemy Attack):** When the blue intelligence effort, which has been started in the last step, is continued, a planned red cyber attack is uncovered. This determines the parameters of table 6 also for Red. The new information turns out to be invaluable for Blue. Since the vulnerability going to be exploited by Red has become clear, an approach for patching the own force elements can be developed well in advance. This specifies the values of the parameters of table 7 for Blue as well. The parameter values describing the red malware attack are as follows:  $\Delta t_{r,\text{att}} = 2.5$ ,  $\Delta t_{r,\text{mal}} = 5.0$ ,  $\alpha_r = 0.5$ . The red malware propagates across the blue force with  $R_b(0) = 0.75N_b(0)$ ,  $S_b(0) = 0.25N_b(0)$ ,  $\beta_b = 0.5$ ,  $\eta_b = 0.5$ . For the countermeasures mounted by Blue it holds  $\Delta t_{b,\text{pat}} = -0.25$ ,  $\gamma_b = 0.5$ ,  $\tilde{\gamma}_b = 0.5\gamma$ .

**Step 5 (Enemy Recovery):** Despite of all blue efforts, Red can still win the outcome as bottom line (see figure 5, second last row). His chances of success depend on a fast and efficient recovery from the blue cyber attack. Accordingly, Blue tries to hamper the development of an efficient patch by Red. This is realized successfully. The parameters of table 7 are now also given for Red, which removes the last uncertainties. We get  $\Delta t_{r,\text{pat}} = 45.0$ ,  $\gamma_r = 0.2$ ,  $\tilde{\gamma}_r = 0.005\gamma_r$  as characterization of the red countermeasures. The fast infection of red force elements together with the slow patch rate of infected systems maximizes the effect of the blue malware attack. The analysis of the given situation (and uncertainty) sequence is organized in the following way. In section 5.2, the risk in the various stages of the sequence is determined. After demonstrating the principal applicability and usefulness of the framework, the value of various contributions to the framework is shown. This concerns the underlying model in section 5.3, the effectiveness of random resp. optimized cyber actions in section 5.4 resp. 5.5, and, finally, the extension from point estimates to the inclusion of uncertainties in section 5.6.

## 5.2 Risk Assessment Results

About 100000 Monte-Carlo simulation runs were executed for each step of the uncertainty sequence. The simulation runs were stopped as soon as the change of all compartment levels was smaller than  $1.0 \cdot 10^{-5}$  for a simulation time interval equal to 1. Figure 5 gives the histograms of the observables  $\Delta N$ ,  $\Delta D$ , and  $L_b$  assessing the simulation outcomes for each step of the complete uncertainty sequence.

In the histograms, the variation of outcomes is significantly reduced as soon as the kinetic parameters are fixed after step 1. Much more prominent cyber effects can be expected for cyber actions being optimized concerning their effect on kinetic combat (see section 5.5). The

small number ( $2/7 \cdot N_b$ ) of blue force elements being susceptible to the red malware attack also contributes to the small scale of cyber effects. The losses  $L_b$  have a distinct peak close to zero only in the start situation. In the step 'force selection', a now even more pronounced peak is located at  $L_b \approx 0.1$ . Later, in the step 'enemy attack', the losses could be reduced further. Simultaneously, the peak is located from now on at  $L_b \approx 0.06$ . This change notices its coming by a corresponding distortion of the outcome distribution in the intermediate step 'cyber attack'. Similar variations can be detected in  $\Delta N$  and  $\Delta D$ .

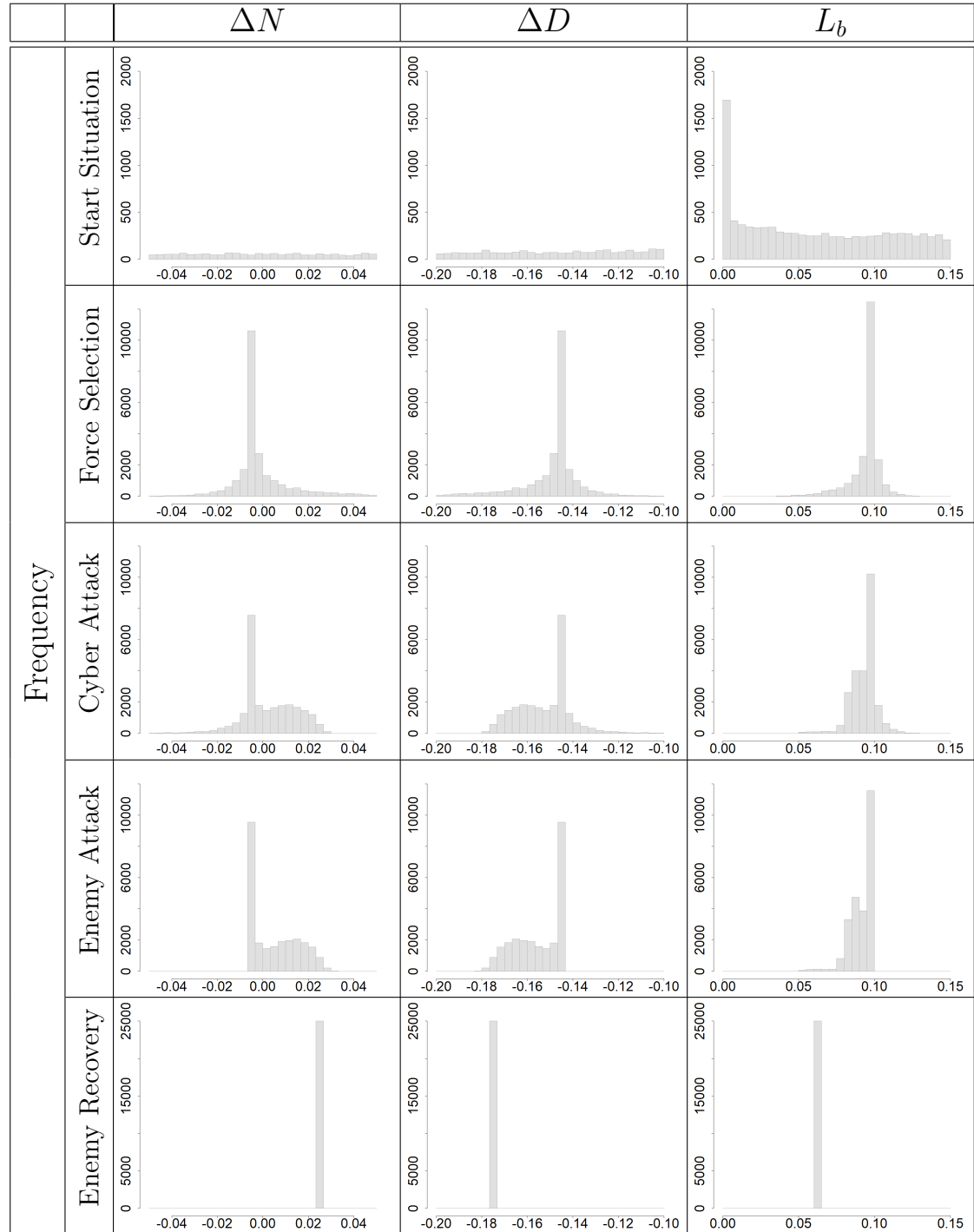


Figure 5: Statistics of the outcomes for the given uncertainty sequence. The outcomes are characterized by the observables  $\Delta N$ ,  $\Delta D$ , and  $L_b$ .

Sequence Step	$\text{mean}(\Delta N)$	$\text{mean}(\Delta D)$	$\text{mean}(L_b)$	$\text{var}(\Delta N)$	$\text{var}(\Delta D)$	$\text{var}(L_b)$
Start Situation	0.013	-0.016	0.292	$2.14 \cdot 10^{-1}$	$1.34 \cdot 10^{-1}$	$6.54 \cdot 10^{-1}$
Force Selection	-0.001	-0.149	0.095	$2.48 \cdot 10^{-4}$	$2.48 \cdot 10^{-4}$	$1.06 \cdot 10^{-4}$
Cyber Attack	0.002	-0.152	0.093	$1.71 \cdot 10^{-4}$	$1.71 \cdot 10^{-4}$	$7.50 \cdot 10^{-5}$
Enemy Attack	0.005	-0.155	0.091	$9.66 \cdot 10^{-5}$	$9.66 \cdot 10^{-5}$	$5.55 \cdot 10^{-5}$
Enemy Recovery	0.024	-0.175	0.063	0.000	0.000	0.000

Table 8: Mean and variance of the observables  $\Delta N$ ,  $\Delta D$ , and  $L_b$  for the given uncertainty sequence. The risk  $\mathcal{R}$  associated with a sequence step is given by  $\mathcal{R} = \text{mean}(L_b)$ .

Sequence Step	Strong Wins	Weak Wins	Weak Losses	Strong Losses
Start Situation	0.413	0.098	0.103	0.385
Force Selection	0.265	0.000	0.734	$2.0 \cdot 10^{-4}$
Cyber Attack	0.482	0.000	0.518	$1.0 \cdot 10^{-4}$
Enemy Attack	0.545	0.000	0.455	0.000
Enemy Recovery	1.000	0.000	0.000	0.000

Table 9: The fractions of wins and losses — considered from the perspective of Blue — along the given sequence of decreasing uncertainty about the expected combat situation.

As a supplement, table 8 gives means and variances. The small size of its expeditionary force is a clear disadvantage for Blue. After fixing force sizes and kinetic parameters in step 2 of the uncertainty sequence, Blue will in fact even typically lose the battle according to  $\text{mean}(\Delta N) \approx -0.001$ . Simultaneously, the higher kinetic effectiveness of Blue leads to significantly higher losses of Red in the mean — from  $\text{mean}(\Delta D) \approx -0.016$  in step 1 of the uncertainty sequence to  $\text{mean}(\Delta D) \approx -0.149$  in step 2. The continuous decrease of  $\text{mean}(\Delta D)$  resp.  $\mathcal{R} = \text{mean}(L_b)$  in later steps indicates that Blue makes better progress in exploiting the cyber aspects of the situation than Red. The decrease of  $\text{mean}(\Delta D)$  is accompanied with an increase of  $\text{mean}(\Delta N)$ . Starting with step 3, the value of  $\text{mean}(\Delta N) \approx 0.002$  is back in the positive range and increases further to  $\text{mean}(\Delta N) \approx 0.024$  in step 5. Concerning the variances, the numbers drop to a value in the range  $10^{-4} - 10^{-5}$  in step 2 ‘force selection’, continuously decreasing further in course of the following steps. Fixing the force sizes to comparatively small values limits the ranges of the observables  $\Delta N$ ,  $\Delta D$ , and  $L_b$ , which contributes to the initial drop of the variances.

The fractions of wins and losses are shown in table 9. Blue has cyber superiority from the beginning, and significantly higher kinetic effectiveness starting with step 2 of the uncertainty sequence. Accordingly, weak wins and strong losses become very rare — the overall technical superiority of Blue and the only moderately larger force of Red make it unlikely that the losses of Blue are higher than the losses of Red. The potential of red options causes a clear drop of the number of strong wins in step 2. Blue demonstrates a clear recovery, however, with a significantly increasing fraction of strong wins along the remaining steps of the uncertainty sequence.

Figure 5 shows only a small part of the histograms of the observables  $\Delta N$ ,  $\Delta D$ , and  $L_b$ . The complete picture for the start situation of the uncertainty sequence is provided in figure 6. The distribution of  $\Delta D$  has a pronounced peak close to  $\Delta D \approx 0$  contrary to  $\Delta N$ . This preference of small values may be caused by a cancellation effect. Typically, both winner and loser will suffer losses, whereas the loser has no surviving force elements at all. Accordingly, the difference  $\Delta D$  of the losses of the opponents will typically cancel out large numbers. For  $\Delta N$  representing the difference of survivors, such a cancellation effect does not occur.

### 5.3 Influence of the Model

Modifications of the model  $M$  representing the given situation may lead to distinct changes of the results. For a demonstration, table 10 compares the model of section 5 (designated as ‘gen’)

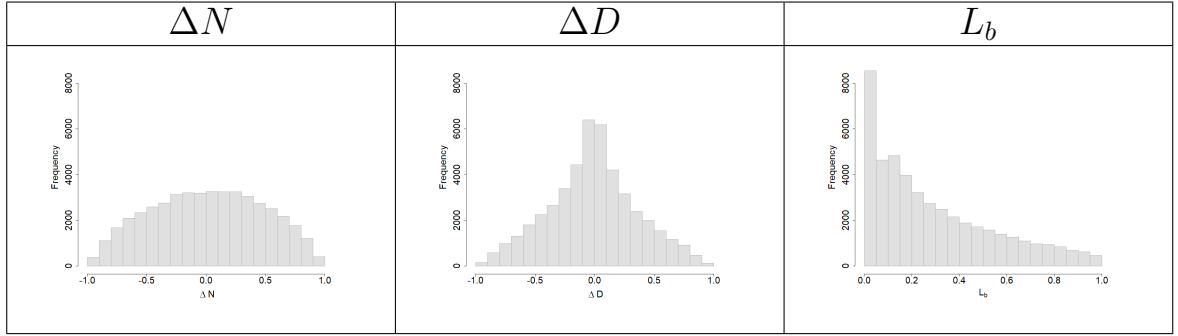


Figure 6: Histograms of the values of the observables  $\Delta N$ ,  $\Delta D$ , and  $L$  for the start situation of the uncertainty sequence.

and the slightly simpler model of Yildiz [60] (designated as 'ref') based on the means of the observables  $\Delta N$ ,  $\Delta D$ , and  $L_b$ . Due to the explicit representation of the malware attack in (8), the model of Yildiz can only essentially, but not fully, be embedded in (8). Taking this restriction into account, a scenario  $x \in X$  can be approximatively mapped to the model of Yildiz by applying the parameter settings  $\alpha = 1$ ,  $\Delta t_{\text{mal}} = 1$ ,  $p, q = 1$ ,  $\tilde{\gamma} = \gamma$ , and  $\Delta t_{\text{att}}, \Delta t_{\text{pat}} = 0$ .

The differences between the results of 'gen' and 'ref' are notable in some stages of the uncertainty sequence. The largest difference can be found with the predicted blue losses at the end of the sequence —  $\mathcal{R} = \text{mean}(L_b) \approx 0.064$  for 'gen' vs.  $\mathcal{R} = \text{mean}(L_b) \approx 0.112$  for 'ref'. Beyond that,  $\text{mean}(\Delta N) < 0$  for 'gen' and  $\text{mean}(\Delta N) > 0$  for 'ref' in step 2 leads to a win/loss classification mismatch (at least in the average).

We can state that using a refined and more detailed model  $M$  may have notable consequences for the analysis results. The proposed framework offers support by allowing to choose the most suitable model  $M \in \mathcal{M}$  instead of using a fixed single model. The results for point estimates also contained in table 10 are discussed in section 5.6.

Sequence Step	Uncertainties?	mean( $\Delta N$ )		mean( $\Delta D$ )		mean( $L_b$ )	
		gen	ref	gen	ref	gen	ref
Start Situation	sampling	0.013	0.011	-0.016	-0.014	0.292	0.338
	point estimate	0.006	0.020	-0.010	-0.024	0.447	0.525
Force Selection	sampling	-0.001	0.032	-0.149	-0.183	0.095	0.116
	point estimate	-0.004	0.032	-0.146	-0.182	0.097	0.117
Cyber Attack	sampling	0.001	0.034	-0.152	-0.185	0.093	0.113
	point estimate	-0.003	0.032	-0.147	-0.182	0.097	0.116
Enemy Attack	sampling	0.006	0.039	-0.156	-0.189	0.091	0.109
	point estimate	-0.002	0.035	-0.148	-0.185	0.096	0.113
Enemy Recovery	sampling	0.025	0.037	-0.175	-0.187	0.064	0.112
	point estimate	0.025	0.037	-0.175	-0.187	0.064	0.112

Table 10: Importance of the modeling details and of the inclusion of uncertainties.

## 5.4 Influence of Random Cyber Actions

For assessing the influence of cyber combat, results reached with one- or two-sided cyber support are compared with results of pure kinetic scenarios. Corresponding scenario classes 'gen' (two-sided cyber warfare), 'cyb' (one-sided cyber warfare), and 'kin' (without cyber warfare), which define subsets of the overall universe of possible situations with help of parameter constraints, are given in table 11. As a first application, the simulation outcomes for the start situation of the

Id	Parameter Settings	Designation	Description
gen	-	General case, i.e. two-sided cyber support	No additional constraints
cyb	$\eta_b = 1$	One-sided cyber support	The blue side is not affected by malware, i.e. Red is fighting only at the kinetic level
kin	$\eta_b, \eta_r = 1$	Pure Lanchester case	Pure kinetic combat without cyber component at all

Table 11: List of scenario classes.

Win/Loss Class	mean( $\Delta N$ )			mean( $\Delta D$ )			mean( $L_b$ )		
	gen	cyb	kin	gen	cyb	kin	gen	cyb	kin
Strong kinetic superiority	0.423	0.431	0.415	-0.322	-0.331	-0.315	0.145	0.137	0.153
Weak kinetic superiority	0.282	0.295	0.265	0.124	0.112	0.142	0.325	0.314	0.342
Weak kinetic inferiority	-0.238	-0.226	-0.260	-0.165	-0.176	-0.143	0.198	0.196	0.205
Strong kinetic inferiority	-0.406	-0.398	-0.423	0.295	0.286	0.312	0.455	0.454	0.460

Table 12: The means of the observables  $\Delta N$ ,  $\Delta D$ , and  $L_b$  for the start situation of the given uncertainty sequence for the scenario classes 'gen', 'cyb', and 'kin'.

uncertain sequence. are broken down to the four kinetic win/loss classes defined in definition 4.2 in table 12. As one may expect,  $\Delta N$  decreases along the sequence 'strong kinetic superiority', 'weak kinetic superiority', 'weak kinetic inferiority', 'strong kinetic inferiority'. This holds for the scenario classes 'gen', 'cyb', and 'kin' likewise. For  $\Delta D$ , the values are correspondingly increasing with the two middle positions interchanged. According to the definition of weak kinetic inferiority with  $\Delta D < 0$  resp. superiority with  $\Delta D > 0$ , the risk for Blue is significantly higher in situations with weak kinetic superiority than in situations with weak kinetic inferiority. As expected, Blue profits from one-sided cyber capabilities in the scenario class 'cyb'. The losses are smaller and the fraction of surviving force elements higher when compared to scenario classes 'gen' and 'kin'. Situations, in which the winning side changes due to the usage of malware, are of special interest. Table 13 takes up this issue. As expected, malware can turn around a situation. Strong wins are possible for all kinetic win/loss classes for both 'gen' and 'cyb'. Cyber support is obviously able to compensate kinetic inferiority. Since one-sided cyber support is a 'true' support — the situation cannot worsen by the usage of malware impeding hostile force elements — some transitions of the win/loss classification are excluded. Kinetic superiority, for example, cannot lead to lost outcomes anymore. Furthermore, strong kinetic superiority in 'cyb' assures a strong win. Thus, a larger number of winning changes can be observed for the scenario class 'cyb' than for 'gen'.

## 5.5 Influence of Optimized Cyber Actions

In the considered example, cyber support leads to fundamental changes of the outcome (see table 13) only in a comparatively small number of cases. This is partially caused by a randomized parameterization of cyber actions. Unexpected frictions or technical breakthroughs, the hardly predictable time required for developing malware and patches, and unforeseen activities of the opponent motivate this simplification. Notwithstanding, military forces will try to exploit any situation to their own advantage in the best possible way. Accordingly, one may expect some kind of optimization in practice. We will thus evaluate its potential in the following. At first, we take a closer look at the changes of the outcomes due to cyber-related actions in dependence on their

Win/Loss Class	Strong Wins		Weak Wins		Weak Losses		Strong Losses	
	gen	cyb	gen	cyb	gen	cyb	gen	cyb
Strong kinetic superiority	0.980	1.000	0.009	0.000	0.008	0.000	0.003	0.000
Weak kinetic superiority	0.085	0.093	0.891	0.907	0.000	0.000	0.023	0.000
Weak kinetic inferiority	0.071	0.075	0.000	0.000	0.891	0.925	0.037	0.000
Strong kinetic inferiority	0.015	0.015	0.012	0.016	0.023	0.025	0.950	0.944

Table 13: The fractions of wins and losses (from the perspective of Blue) in the start situation of the given uncertainty sequence.

parameterization. For this purpose, we define  $\Delta\Delta N := \Delta N(x) - \Delta N(g_{\text{kin}}(x))$  and analogously  $\Delta\Delta D, \Delta L_b$ .

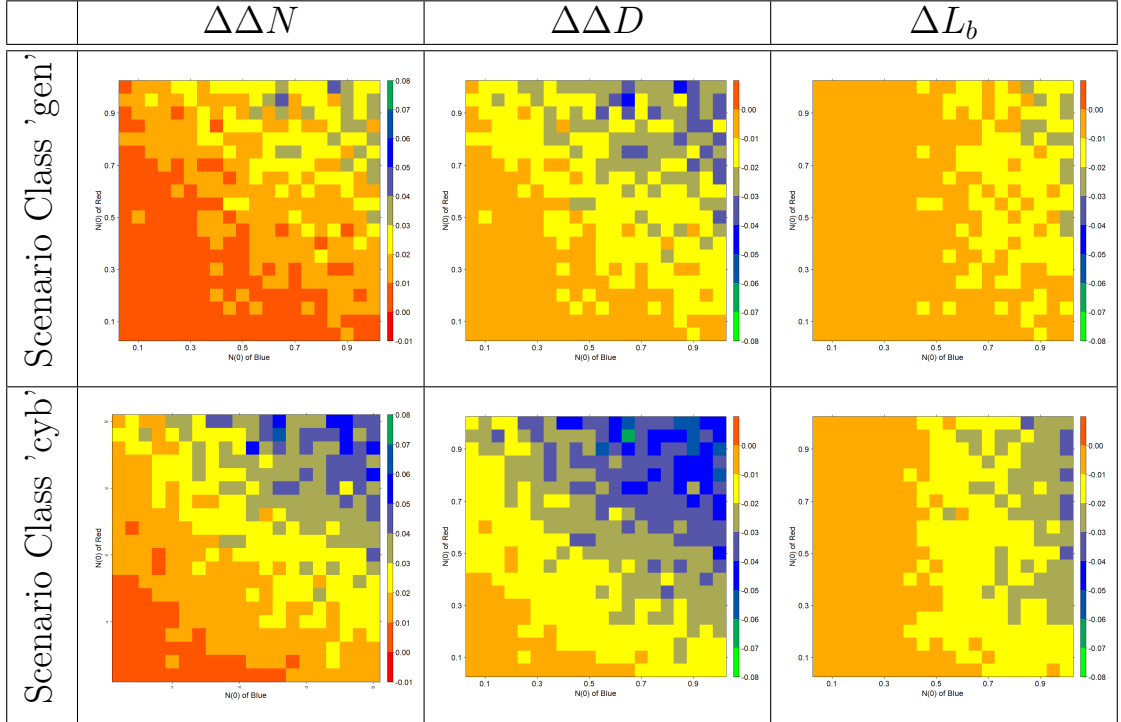


Figure 7: Cyber support as an option for compensating kinetic inferiority. The heatmaps show the means of  $\Delta\Delta N$ ,  $\Delta\Delta D$ , and  $\Delta L_b$  dependent on the force sizes  $N_b(0)$  vs.  $N_r(0)$  for one- and two-sided cyber support ('cyb' and 'gen').

Figure 7 shows the means of  $\Delta\Delta N$ ,  $\Delta\Delta D$ , and  $\Delta L_b$  dependent on the initial force sizes  $N_b(0)$ ,  $N_r(0)$ . The changes are distinctively larger for one-sided cyber support (scenario class 'cyb') than for two-sided support (scenario class 'gen'). More important, some settings of the parameters  $N_b(0)$ ,  $N_r(0)$  give higher chances of a large change than others. This observation is supported by figure 8, which shows the influence of infection rate  $\beta_b$  and timing  $\Delta t_{b,\text{att}}$  on  $\Delta\Delta N$  resp.  $\Delta L_b$ . Though in large regions of the parameter space the influence is typically small or even neglectable,  $\Delta\Delta N$  and  $\Delta L_b$  can reach large values in others. Summing up, we can confirm comparatively small effects of randomly configured cyber actions, but we can expect potentially large effects on the outcome with appropriately refined parameter values.

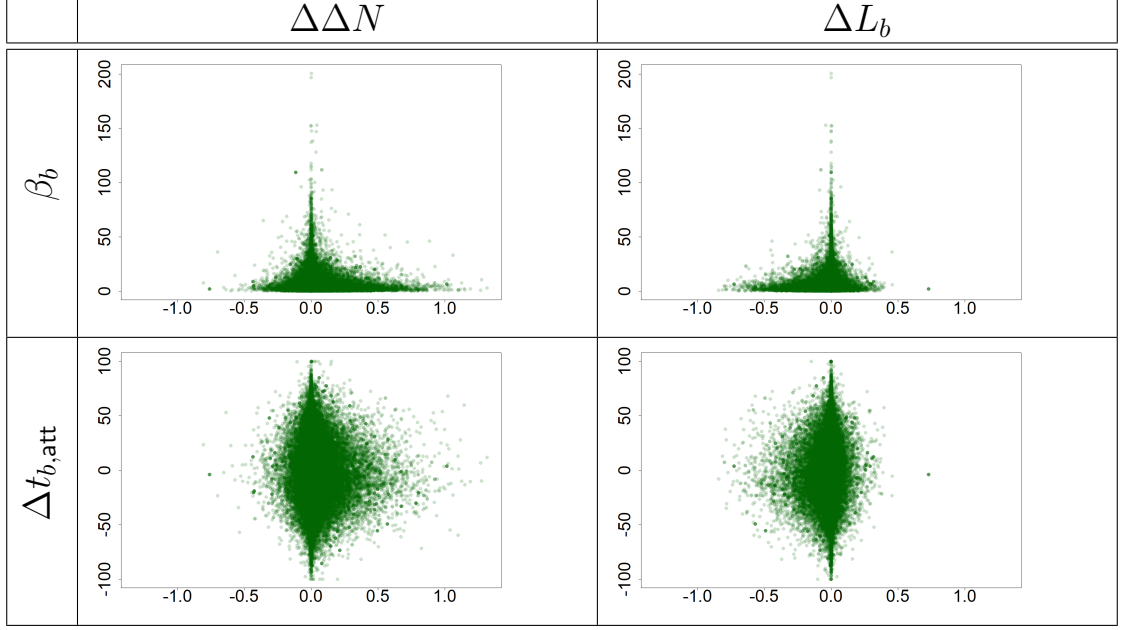


Figure 8: Cyber support may change the outcome of kinetic combat. The scatterplots demonstrate the influence of the input parameter  $\beta_b$  resp.  $\Delta t_{b,att}$  on the magnitude of the changes  $\Delta\Delta N$  and  $\Delta L_b$  in the scenario class 'gen'.

Definition of Subregions of the Scenario Space 'gen'				
gen0	$p, q \in [0, \infty)$	$\delta_b, \delta_r \in [0, \infty)$		
gen1	$[0, 7]$	$[0, 3.5]$		
gen2	$[0, 5]$	$[0, 2.5]$		
gen0	$\beta_b, \beta_r \in [0, \infty)$	$\eta_b \in [0, 1]$	$\eta_r \in [0, 1]$	
gen1	$[0, 17.5]$	$[0.3, 1]$	$[0, 0.7]$	
gen2	$[0, 12.5]$	$[0.5, 1]$	$[0, 0.5]$	
gen0	$\Delta t_{b,att} \in (-\infty, \infty)$	$\Delta t_{r,att} \in (-\infty, \infty)$	$\Delta t_{b,pat} \in (-\infty, \infty)$	$\Delta t_{r,pat} \in (-\infty, \infty)$
gen1	$[-80, 120]$	$[-120, 80]$	$[-90, 60]$	$[-60, 90]$
gen2	$[-40, 80]$	$[-80, 40]$	$[-60, 30]$	$[-30, 60]$
gen0	$R_b(0) \in [0, N_b(0)]$	$R_r(0) \in [0, N_r(0)]$	$\gamma_b, \gamma_r \in [0, 1]$	$\gamma'_b, \gamma'_r \in [0, 1]$
gen1	$[0, 1]$	$[0, 0.35]$	$[0, 0.7]$	$[0, 0.35]$
gen2	$[0.25, 1]$	$[0, 0.25]$	$[0, 0.5]$	$[0, 0.25]$

Table 14: Restrictions of the scenario space of the start situation of the given uncertainty sequence to specific subregions. Whereas the scenario set 'gen0' covers the complete scenario space, the scenario sets 'gen1', 'gen2' are restrictions of 'gen0' subject to the indicated constraints. For the parameters  $N(0)$ ,  $\Delta t_{mal}$ , and  $\alpha$ , no additional constraints are raised.

The influence of appropriately chosen cyber action parameters should be examined more closely. For this purpose, subregions 'gen0', 'gen1' of the scenario space of the start situation of the uncertainty sequence are defined in table 14. The influence of cyber actions is clearly visible in table 15 with the number of outcomes, which belong to a different win/loss class (table columns) than the corresponding pure kinetic situation (table rows). The fraction of strong wins increases from 'gen0' to 'gen1' in all four kinetic win/loss classes significantly. The increase in case of weak kinetic inferiority could even be considered as dramatic: From 0.071 (for 'gen') resp. 0.077 (for 'cyb') to 0.750 (for 'gen' and 'cyb'). Remarkable as well is the increase of strong wins for strong kinetic inferiority: From 0.015 resp. 0.016 to 0.141. The small differences between 'gen' and 'cyb' may be caused by the assumption of cyber superiority for Blue from the beginning. Based on these observations, we conclude that the small number of changing win/loss classifications



Win/Loss Class	Scenario Set	Strong Wins		Weak Wins		Weak Losses		Strong Losses	
		gen	cyb	gen	cyb	gen	cyb	gen	cyb
Strong kinetic superiority	gen0	0.980	1.000	0.009	0.000	0.008	0.000	0.003	0.000
	gen1	0.987	1.000	0.008	0.000	0.005	0.000	0.000	0.000
	gen2	1.000	1.000	0.000	0.000	0.000	0.000	0.000	0.000
Weak kinetic superiority	gen0	0.085	0.096	0.891	0.904	0.000	0.000	0.023	0.000
	gen1	0.139	0.141	0.846	0.859	0.000	0.000	0.015	0.000
	gen2	0.172	0.172	0.828	0.828	0.000	0.000	0.000	0.000
Weak kinetic inferiority	gen0	0.071	0.077	0.000	0.000	0.891	0.923	0.037	0.000
	gen1	0.203	0.206	0.000	0.000	0.748	0.794	0.048	0.000
	gen2	0.750	0.750	0.000	0.000	0.250	0.250	0.000	0.000
Strong kinetic inferiority	gen0	0.015	0.016	0.012	0.016	0.023	0.026	0.950	0.942
	gen1	0.041	0.042	0.025	0.029	0.052	0.052	0.882	0.877
	gen2	0.141	0.141	0.047	0.055	0.055	0.055	0.758	0.750

Table 15: The influence of cyber actions summarized as fractions of wins and losses for the scenario sets 'gen0', 'gen1', 'gen2' defined in table 14.

due to cyber actions in table 13 seems indeed be caused by the random parameterization of the cyber actions.

## 5.6 Influence of Uncertainties

The inclusion of uncertainties resulting from missing knowledge is an important contribution towards practicability. It requires the consideration of a whole set of scenarios instead of only a single one. The statistical properties of the corresponding set of outcomes provides information not accessible otherwise. Its value results from the incompatibility between statistics and dynamics. This means that the typical outcome does not necessarily coincide with the so-called point estimate, i.e. the outcome of the typical scenario, as demonstrated in table 10.

The point estimate of a Monte-Carlo design space  $(X, \text{Prob})$  is defined as follows. According to section 4.1, a scenario  $x \in X$  is the Cartesian product  $x = \times_k x_k$  of the model parameters (see table 1) and of the initial values of equation system (13). If we neglect the few dependencies between the parameters  $x_k$  in the example, the probability distribution  $\text{Prob}$  is decomposable as well according to  $\text{Prob} = \times_k \text{Prob}_k$ . This facilitates the definition of the 'typical' scenario as  $x_{\text{Prob}} := \times_k \text{mean}(x_k)$ . Then, the *point estimate* of  $(X, \text{Prob})$  is given as  $\text{sim}(x_{\text{Prob}})$ .

The differences between risk assessments with inclusion of uncertainties (indicated by term 'sampling', being the mean of all sampled outcomes) and corresponding 'point estimates' in table 10 can typically be neglected for small uncertainties. In the case of large uncertainties, however, the deviation may be significant. This is demonstrated by the losses  $L_b$  in the start situation of the example. Beyond that, modified win/loss classifications due to the inclusion of uncertainties cannot be excluded. In the table, this occurs in the steps 'cyber attack' and 'enemy attack' due to different signs of  $\text{mean}(\Delta N)$ .

## 6 Application of the framework

After the presentation of the proposed framework, some remarks about its application should be made. This especially concerns, how information about the situation, which should be analyzed, is extracted and handed over to the framework. With regard to ensuring an adequate representation of the situation by the model used in the framework, we refer to the related discussions in the sections 2 and 3. In the following, we will additionally address the quantitative determination of the values of the model parameters. We will also discuss, how the results computed

with help of the framework can be utilized for achieving better decisions. These considerations demonstrate that the framework is not only scientifically correct but also practically useful.

## 6.1 Providing the Inputs of the Framework

In order to apply the framework, the parameter values characterizing the scenario(s) to be processed with the framework model have to be determined [48]. This translates the maybe quite abstract properties of the real-world force elements into numeric input of the model. For the purpose of our discussion, we will again focus on the example in section 5.

The values can be determined by measurement executed either in reality or in corresponding computer-based simulation experiments [26]. The latter is especially of interest, if the values have to be known *before* the situation unfolds in reality. Applying these usually quite elaborated simulation models also to risk assessment purposes cannot be recommended, though; their large runtime and lack of important theoretical properties (see section 2.7 below) exclude such usage. Measurement errors can be taken into account as uncertainties in accordance with the design of the framework.

The values of the parameters  $\delta$ ,  $p$ ,  $q$  of the Lanchester component — resp. their statistics [13,34] due to their dependence on the specific circumstances of an engagement [1] — can be determined by fitting a Lanchester model to the dynamic behavior of a discrete event simulation model [54]. The parameter  $\eta$  is accessible analogously based on the effects of a malware infection on force element capabilities. The framework integrates value statistics seamlessly as value uncertainties. Concerning the parameters  $\beta$  and  $\gamma$  (resp.  $\tilde{\gamma}$ ) of the SIR component, we follow [22]. According to the differential equation system (13), the infection rate  $\beta$  can be determined by measuring the number  $I_{\Delta T}$  of new malware infections in a (small) time period  $\Delta T$  based on  $I_{\Delta T} = \beta SIN^{-1} \Delta T$  [25]. An observation of the time period  $\tau$ , in which a force element is infected with malware, immediately gives the recovery rate  $\gamma = \tau^{-1}$  [25, 55, 59]. Alternatively, parameters like  $\beta$  can be determined based on malware properties. According to [62], it holds  $\beta = \xi/O$ , where  $\xi$  is the scanning rate of the malware and  $O$  the size of the scanned subset of potential infection targets. Finally, the values of the parameters  $\Delta t_{\text{att}}$ ,  $\Delta t_{\text{mal}}$ ,  $\Delta t_{\text{pat}}$ , and  $\alpha$  result from decisions of the military leaders. As such, they belong to the what-if part of the application of the framework. They cannot be predicted in a deterministic way.

## 6.2 Applying the Results of the Framework

The framework computes the value of the risk  $R$  associated with a conflict situation  $S$  based on a model  $M \in \mathcal{M}$  of  $S$ . Since we cannot completely rule out unjustified assumptions about the situation at hand in principle, the determination of the value of  $R$  can be sometimes worthless in spite of the correctness of the computation itself. In the end, it depends on the judgement of the user whether the information about  $R$  is considered as valuable. Should this be the case, he also determines how it is then exploited. He may modify the planned course of action and/or decide about actions in order to change the situation  $S$  towards a lower risk value, but he may also choose to still disregard the risk estimate completely. The framework *supports* human decision making, but does not replace it. It is the human decider who selects the scenarios he is especially interested in. He does so by setting the knowledge encoded into the underlying model and into the parameter values in an overall situational context. Analogously, he disposes about the usage of the computed values of risk assigned to these scenarios.

## 6.3 Utility of the Framework

The utility of the framework relates to the quality of the decisions of the military leaders applying it. In this respect, 'quality' means the tendency to avoid situations with a high number of own losses. (Un)Fortunately, such an observation-based utility adjudication is hampered by an insufficient amount of real-world data.

To get around this difficulty, we discuss the utility of the framework resting upon theoretical arguments instead of observations. Without doubt, long-term predictions with inclusion of uncertainties are a task hardly manageable by humans in general. The provision of measures like

the risk  $R$  with help of the framework can thus be considered as highly valuable knowledge, as long as an extensive validation effort supports the correctness of the value of  $R$ . For rationally acting users, the knowledge about  $R$  can thus be viewed as a principal advantage. It simplifies pending decisions by a reduction of existing unknowns. The framework may therefore be judged as practically useful.

## 7 Discussion and Outlook

In the following, we will point out limitations and restrictions of the proposed framework as well as opportunities of future research.

### 7.1 Extension of the Class $\mathcal{M}$ of Models

The faithfulness of situation representations may be increased by extending the underlying class  $\mathcal{M}$  of models due to the additional modeling options. System dynamics components of kinetic combat and of malware propagation more general than utilized in the model class  $\mathcal{M}$  are proposed in e.g. [4, 6]. Especially the Lanchester component may profit from such a generalization. The basic Lanchester model assumes, for example, that incapacitated opponents must be known at once, so that fire is distributed only against active opponents [27]. For being more realistic, the compartment  $D$  representing the already destroyed elements may attract a certain fraction of the fire of the opposing force as well.

The investigation of further examples will clarify, whether a risk analysis of more detailed — especially heterogeneous — models can proceed according to the template given by section 5. Tractability may be a possible concern, since more details will usually be accompanied with a higher number of parameters. It seems hardly feasible to determine the accurate values of a large number of model parameters, though. Significant uncertainties will be the result, which in turn require the execution of a large number of Monte Carlo simulation runs for assuring a sufficient statistical significance of the computed risk value. It may thus be difficult to make straightforward use of the details of a more elaborated model without corresponding knowledge about the values of the model parameters.

The restriction of  $\mathcal{M}$  to deterministic models should be abandoned, as soon as small force numbers play a role. Such a situation occurs in the start phase of an infection with self-replicating malware, in which the number of infected elements is small, and for overall small forces [12]. Then, stochastic fluctuations eventually influencing the system dynamics will not cancel out anymore. The extension of  $\mathcal{M}$  towards stochastic models may thus contribute to the validity of results. A stochastic model dynamics can be perfectly integrated in the Monte Carlo approach of the framework.

### 7.2 Improving the Utility of the Framework

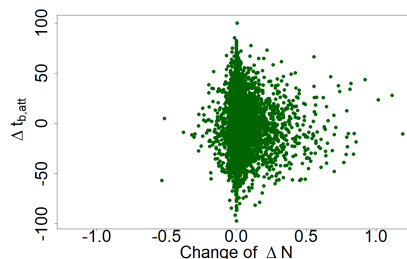


Figure 9: The distribution of  $\Delta\Delta N$  dependent on  $\Delta t_{b,att}$  indicates, which values of  $\Delta t_{b,att}$  may cause large cyber effects.

The proposed framework can be applied for other purposes than decision support as well. Based on the calculated risk, various attack methods, infection mechanisms, propagation pathways,

and countermeasures can be analyzed and compared with each other. This permits an identification of preferable system design principles. Experimentation with the consequences of different knowledge (or assumptions) about a given situation is enabled.

Beyond that, the framework can help for configuring the cyber actions. Let us take a look at the timing  $\Delta t_{b,\text{att}}$  of the blue cyber attack in the analyzed example. In the step 'Cyber Attack' of the uncertainty sequence, the kinetic aspects are already fixed. The parameter settings  $R_r(0) \approx 0.15$ ,  $\beta_r \approx 1.75$  may also have already become known. For scenarios satisfying the given technical malware parameters, the changes of  $\Delta N$  dependent on the timing  $\Delta t_{b,\text{att}}$  of the blue malware attack are distributed as shown in figure 9. According to the plot, we may eventually expect a large advantageous influence on the outcome of the combat for  $\Delta t_{b,\text{att}} \approx -15.0$ . There, the changes of  $\Delta N$  reach their maximum both absolutely and in the mean though several singular data points representing large positive changes of  $\Delta N$  can also be observed for  $\Delta t_{b,\text{att}} > 0$ . Hence, the parameter setting  $\Delta t_{b,\text{att}} \approx -15.0$  seems to be a good working hypothesis. As can be seen in section 5.2, the situation indeed has been improved with this choice. We are not going to discuss these additional benefits further, though. They may be topic of future research.

## 8 Acknowledgements

The authors are grateful for many helpful remarks provided by Filipa Campos-Viola, Elisa Canzani, Stefan Hahndel, Thomas Rieth, Harald Schaub, Christine Schwarz-Hemmert and Iris Berthold. Additionally, we want to thank Simon Hurst for his support for validating the implementation of the computational model.

## References

- [1] Clinton J Ancker Jr and Antranig V Gafarian. The validity of assumptions underlying current uses of lanchester attrition rates. *Naval Research Logistics (NRL)*, 34(4):505–533, 1987.
- [2] Michael R Bathe and Kenneth R McNaught. Development of a combat model with a mini-battle structure. Technical report, ROYAL MILITARY COLL OF SCIENCE SHRIVENHAM (UNITED KINGDOM) SYSTEMS, 1989.
- [3] James O Berger. *Statistical decision theory and Bayesian analysis*. Springer Science & Business Media, 2013.
- [4] Oscar M. Bull. System dynamics applied to combat models (Lanchester laws). In *The 28th International Conference of the System Dynamics Society*. System Dynamics Society, 2010.
- [5] William R Burns and Drew Miller. Improving dod adaptability and capability to survive black swan events. *JFQ*, 2014.
- [6] Vittoria Colizza, Marc Barthélemy, Alain Barrat, and Alessandro Vespignani. Epidemic modeling in complex realities. *Comptes rendus biologiques*, 330(4):364–374, 2007.
- [7] Keith Conrad. Probability distributions and maximum entropy. *Entropy*, 6(452):10–36, 2004.
- [8] Christian Czosseck, Rain Ottis, and Anna-Maria Talihärm. Estonia after the 2007 cyber attacks: Legal, strategic and organisational changes in cyber security. *International Journal of Cyber Warfare and Terrorism*, 1(1):24–34, 2011.
- [9] Dancho Danchev. Coordinated Russia vs. Georgia cyberattack in progress. *ZDNet*, 2008.
- [10] Sumanta Kumar Das. Fitting heterogeneous Lanchester models on the Kursk campaign. *preprint arXiv:1903.06666*, 2019.

- [11] Paul K Davis and Donald Blumenthal. The base of sand problem: A white paper on the state of military combat modeling. Technical report, Defense Advanced Research Projects Agency, Arlington, 1991.
- [12] Angel Martín del Rey. Mathematical modeling of the propagation of malware: A review. *Security and Communication Networks*, 8(15):2561–2579, 2015.
- [13] John A Dinges. Exploring the validation of lanchester equations for the battle of kursk. Technical report, Naval Postgraduate School, Monterey CA, 2001.
- [14] Joachim Draeger. Roadmap to a unified treatment of safety and security. In *Proceedings of the 10th IET System Safety and Cyber-Security Conference*. IET, 2015.
- [15] Joachim Draeger and Stefan Hahndel. Formalized risk assessment for safety and security. *preprint arXiv:1709.00567v2*, 2017.
- [16] Romney B Duffey. Dynamic theory of losses in wars and conflicts. *European Journal of Operational Research*, 261(3):1013–1027, 2017.
- [17] Joseph H Engel. A verification of Lanchester’s law. *Journal of the Operations Research Society of America*, 2(2):163–171, 1954.
- [18] Ronald D Fricker Jr. Attrition models of the Ardennes campaign. *Naval Research Logistics*, 45(1):1–22, 1998.
- [19] Kenneth Geers. *Cyber war in perspective: Russian aggression against Ukraine*. NATO Cooperative Cyber Defence Centre of Excellence, 2015.
- [20] Robert Ghanea-Hercock. Why cyber security is hard. *Georgetown Journal of International Affairs*, pages 81–89, 2012.
- [21] Rebecca Grant. Airpower made it work. *Air Force Magazine*, 82(11):30–37, 1999.
- [22] Kristopher Joseph Hall. *Thwarting network stealth worms in computer networks through biological epidemiology*. PhD thesis, Virginia Tech, 2006.
- [23] Edward F Halpin, Philippa Trevorrow, David Webb, and Steve Wright. *Cyberwar, netwar and the revolution in military affairs*. Springer, 2006.
- [24] Dean S Hartley III and Robert L Helmbold. Validating Lanchester’s square law and other attrition models. *Naval Research Logistics*, 42(4):609–633, 1995.
- [25] Soodeh Hosseini, Mohammad Abdollahi Azgomi, and Adel Rahmani Torkaman. Agent-based simulation of the dynamics of malware propagation in scale-free networks. *Simulation*, 92(7):709–722, 2016.
- [26] Bonan Hou, Yiping Yao, Bing Wang, and Dongsheng Liao. Modeling and simulation of large-scale social networks using parallel discrete event simulation. *Simulation*, 89(10):1173–1183, 2013.
- [27] Wayne P Hughes Jr. Two effects of firepower: Attrition and suppression. *Military Operations Research*, pages 27–35, 1995.
- [28] Edwin Jaynes. Information theory and statistical mechanics. *Physical review*, 106(4):620–630, 1957.
- [29] C.I.O. Kamalu, M.S. Nwakaudu, J.C. Obijiaku, P. Oghome, E. Okoh, and F.N. Uzundu. Regression modeling of Iraq Iran war using Lancaster/Osipov war models. *International Journal of Engineering and Innovative Technology*, 5:1–10, 2016.
- [30] William O Kermack and Anderson G McKendrick. A contribution to the mathematical theory of epidemics. *Proceedings of the Royal Society of London A: Mathematical, Physical and Engineering Sciences*, 115(772):700–721, 1927.

- [31] Moshe Kress. Modeling armed conflicts. *Science*, 336(6083):865–869, 2012.
- [32] Frederick William Lanchester. Mathematics in warfare. *The world of mathematics*, 4:2138–2157, 1956.
- [33] Robert Lee, Michael Assante, and Tim Conway. Analysis of the cyber attack on the ukrainian power grid. *Electricity Information Sharing and Analysis Center (E-ISAC)*, 2016.
- [34] Thomas W Lucas and John A Dinges. The effect of battle circumstances on fitting lanchester equations to the battle of kursk. *Military Operations Research*, pages 17–30, 2004.
- [35] Thomas W Lucas and Turker Turkes. Fitting Lanchester equations to the battles of Kursk and Ardennes. *Naval Research Logistics*, 51(1):95–116, 2004.
- [36] Niall MacKay. Lanchester combat models. *preprint arXiv:math/0606300*, 2006.
- [37] Helmut Martin-Jung. Cyberangriff auf den Bundestag - Für Lücken büßen. *Süddeutsche Zeitung*, 2015.
- [38] Dale McMorrow. Science of cyber-security. Technical report, MITRE corporation, 2010.
- [39] Bimal Kumar Mishra and Gholam Mursalin Ansari. Differential epidemic model of virus and worms in computer network. *IJ Network security*, 14(3):149–155, 2012.
- [40] Bimal Kumar Mishra and Apeksha Prajapati. Modelling and simulation: Cyber war. *Procedia Technology*, 10:987–997, 2013.
- [41] Scott Musman, Aaron Temin, Mike Tanner, Dick Fox, and Brian Pridemore. Evaluating the impact of cyber attacks on missions. In *International Conference on Cyber Warfare and Security*, pages 446–460. Academic Conferences International Limited, 2010.
- [42] Jose Pagliery. Scary questions in ukraine energy grid hack, 2016.
- [43] Sung Y Park and Anil K Bera. Maximum entropy autoregressive conditional heteroskedasticity model. *Journal of Econometrics*, 150(2):219–230, 2009.
- [44] Sancheng Peng, Shui Yu, and Aimin Yang. Smartphone malware and its propagation modeling: A survey. *IEEE Communications Surveys & Tutorials*, 16(2):925–941, 2013.
- [45] Philip J Romero. A new approach for the design and evaluation of land defense concepts. Technical report, Rand Corporation, Santa Monica, CA, 1991.
- [46] Irwin Sandberg. On the mathematical foundations of compartmental analysis in biology, medicine, and ecology. *IEEE transactions on Circuits and Systems*, 25(5):273–279, 1978.
- [47] Harrison C Schramm and Donald P Gaver. Lanchester for cyber: The mixed epidemic-combat model. *Naval Research Logistics*, 60(7):599–605, 2013.
- [48] Artur M Schweidtmann, Jana M Weber, Christian Wende, Linus Netze, and Alexander Mitsos. Obey validity limits of data-driven models. *arXiv preprint arXiv:2010.03405*, 2020.
- [49] Thorsten Severin, Michael Nienaber, and Andrew Heavens. Cyber attack on german parliament still active, could cost millions. 2015.
- [50] Ioannis D Sfikas. Model of warfare. *Journal of Computations & Modelling*, 7(1):99–114, 2017.
- [51] Sekaran Sneha, Lakshmanan Malathi, and R Saranya. A survey on malware propagation analysis and prevention model. *Int. J. Adv. Technology*, 6(148):2–5, 2015.
- [52] Julian Stodd and Emilie Reitz. Black swans: Disruption of power. In *Proceedings of ITSEC*, 12 2017.

- [53] Pei-Chen Sung and Chien-Yuan Su. Using system dynamics to investigate the effect of the information medium contact policy on the information security management. *International Journal of Business and Management*, 8(12):83–96, 2013.
- [54] James G Taylor. Lanchester-type models of warfare. volume ii. Technical report, Naval Postgraduate School, Monterey CA, 1980.
- [55] Thanawat Tiensin, Mirjam Nielen, Hans Vernooij, Thaweesak Songserm, Wantanee Kalpravidh, Sirikan Chotiprasatintara, Arunee Chaisingh, Surapong Wongkasemjit, Karoon Chanachai, Weerapong Thanapongtham, et al. Transmission of the highly pathogenic avian influenza virus h5n1 within flocks during the 2004 epidemic in thailand. *The Journal of infectious diseases*, 196(11):1679–1684, 2007.
- [56] Andreas Tolk. Challenges of combat modeling and distributed simulation. In *Engineering principles of combat modeling and distributed simulation*, pages 1–23. Wiley, 2012.
- [57] Chao Wang, Ke Xu, and Gaoyu Zhang. A SEIR-based model for virus propagation on sns. In *Fourth International Conference on Emerging Intelligent Data and Web Technologies*, pages 479–482. IEEE, 2013.
- [58] Gaute Wangen and Andrii Shalaginov. Quantitative risk, statistical methods and the four quadrants for information security. In *International Conference on Risks and Security of Internet and Systems*, pages 127–143. Springer, 2015.
- [59] Yu Yao, Qiang Fu, Wei Yang, Ying Wang, and Chuan Sheng. An epidemic model of computer worms with time delay and variable infection rate. *Security and Communication Networks*, 2018, 2018.
- [60] Fatih Yıldız. Modeling the effects of cyber operations on kinetic battles. Technical report, Naval Postgraduate School, Monterey, Department of Operations Research, 2014.
- [61] Fatih Yıldız. Modeling the continuous effects of cyber operations on kinetic battles. *Military and Security Studies*, pages 32–37, 2015.
- [62] Cliff C Zou, Don Towsley, and Weibo Gong. On the performance of internet worm scanning strategies. *Performance Evaluation*, 63(7):700–723, 2006.